Journal of Visualized Experiments

Controlled Strain of 3D Hydrogels under Live Microscopy Imaging

--Manuscript Draft--

Article Type:	Methods Article - JoVE Produced Video
Manuscript Number:	JoVE61671R1
Full Title:	Controlled Strain of 3D Hydrogels under Live Microscopy Imaging
Corresponding Author:	Avraham Kolel Tel Aviv University Iby and Aladar Fleischman Faculty of Engineering Tel-Aviv, ISRAEL
Corresponding Author's Institution:	Tel Aviv University Iby and Aladar Fleischman Faculty of Engineering
Corresponding Author E-Mail:	avrahamkolel@mail.tau.ac.il
Order of Authors:	Avraham Kolel, B.A.
	Avishy Roitblat Riba
	Sari Natan
	Oren Tchaicheeyan
	Ayelet Lesman
Additional Information:	
Question	**Response**
Please indicate whether this article will be Standard Access or Open Access.	Standard Access (US$2,400)
Please indicate the **city, state/province, and country** where this article will be **filmed**. Please do not use abbreviations.	Tel-Aviv, Israel
Please confirm that you have read and agree to the terms and conditions of the author license agreement that applies below:	I agree to the Author License Agreement
Please specify the section of the submitted manuscript.	Bioengineering
Please provide any comments to the journal here.	We added an author since the original submission, please include this new author in the publication.

TITLE:

Controlled Strain of 3D Hydrogels under Live Microscopy Imaging

AUTHORS AND AFFILIATIONS:

Avraham Kolel[1], Avishy Roitblat Riba[2], Sari Natan[3], Oren Tchaicheeyan[3], Eilom Saias,[2] Ayelet Lesman[3]

[1]Department of Biomedical Engineering, Faculty of Engineering, Tel-Aviv University, Tel-Aviv, Israel

[2]Department of Material Science and Engineering, Faculty of Engineering, Tel-Aviv University, Tel-Aviv, Israel

[3]School of Mechanical Engineering, Faculty of Engineering, Tel-Aviv University, Tel-Aviv, Israel

KEYWORDS:

Hydrogel, Extracellular matrix, Mechanobiology, Cell mechanics, Mechanical force, External stretching, Fibrous network, Fiber alignment

SUMMARY:

The presented method involves uniaxial stretching of 3D soft hydrogels embedded in silicone rubber while allowing live confocal microscopy. Characterization of the external and internal hydrogel strains as well as fiber alignment are demonstrated. The device and protocol developed can assess the response of cells to various strain regimes.

ABSTRACT:

External forces are an important factor in tissue formation, development, and maintenance. The effects of these forces are often studied using specialized in vitro stretching methods. Various available systems use 2D substrate-based stretchers, while the accessibility of 3D techniques to strain soft hydrogels, is more restricted. Here, we describe a method that allows external stretching of soft hydrogels from their circumference, using an elastic silicone strip as the sample carrier. The stretching system utilized in this protocol is constructed from 3D-printed parts and low-cost electronics, making it simple and easy to replicate in other labs. The experimental process begins with polymerizing thick (> 100 μm) soft fibrin hydrogels (Elastic Modulus of ~100 Pa) in a cut-out at the center of a silicone strip. Silicone-gel constructs are then attached to the printed-stretching device and placed on the confocal microscope stage. Under live microscopy the stretching device is activated, and the gels are imaged at various stretch magnitudes. Image processing is then used to quantify the resulting gel deformations, demonstrating relatively homogenous strains and fiber alignment throughout the gel's 3D thickness (*Z*-axis). Advantages of this method include the ability to strain extremely soft hydrogels in 3D while executing in situ microscopy, and the freedom to manipulate the geometry and size of the sample according to the user's needs. Additionally, with proper adaptation, this method can be used to stretch other types of hydrogels (e.g., collagen, polyacrylamide or polyethylene glycol) and can allow for analysis of cells and tissue response to external forces under more biomimetic 3D conditions.

INTRODUCTION:

Tissue response to mechanical forces is an integral part of a wide range of biological functions, including gene expression[1], cell differentiation[2], and tissue remodeling[3]. Moreover, force-induced changes in the extracellular matrix (ECM) such as fiber alignment and densification can impact cell behavior and tissue formation[4,5,6]. The ECM's fibrous mesh structure has intriguing mechanical properties, such as non-linear elasticity, non-affine deformation and plastic deformations[7,8,9,10,11,12]. These properties impact how cells and their surrounding microenvironment respond to external mechanical forces[13,14]. Understanding how the ECM and tissues respond to mechanical forces will enable progress in the field of tissue engineering and in the development of more accurate computational and theoretical models.

Most common methods to mechanically stretch samples have focused on cell-laden 2D substrates to explore the effects on cell behavior. These include, for example, applying strain to polydimethylsiloxane (PDMS) substrates and analyzing cell reorientation angles in relation to the stretch direction[15,16,17,18,19]. Yet, methods investigating the response of 3D cell-embedded hydrogels to external stretch, a situation that more closely mimics tissue microenvironment, are more limited. Advances toward 3D stretching methods are of particular importance because cells behave differently on 2D substrates when compared to 3D matrices[20]. These behaviors include cellular realignment, protein expression levels, and migration patterns[21,22,23].

Methods and devices that allow for 3D sample stretching include both commercially available[24,25,26,27,28] and those developed for laboratory research[29]. These methods use distensible silicone tubes[30], multi-well chambers[31], clamps[26,32], bioreactors[11,33], cantilevers[34,35,36], and magnets[37,38]. Some techniques generate stretch that locally deforms 3D hydrogels, for example by pulling needles from two single points in the gel[5], while others allow for deformation of the entire bulk of the gel[16]. Moreover, most of these systems focus on analysis of the strain field in the *X*-*Y* plane, with limited information on the strain field in the *Z*-direction. Additionally, only a handful of these devices are capable of microscopic in situ imaging. The main challenge with in situ high-magnification imaging (e.g., confocal microscope) is the limited working distance of a few hundred microns from the objective lens to the sample. Devices that do allow *live* imaging during stretch sacrifice the uniformity of strain in the *Z*-axis or are relatively complex and difficult to reproduce in other laboratories[39,40].

This approach to stretch 3D hydrogels allows for static or cyclical uniaxial strain during live confocal microscopy. The stretching device (referred to as 'Smart Cyclic Uniaxial Stretcher – SCyUS') is constructed using 3D printed parts and low-cost hardware, allowing easy reproduction in other labs. Attached to the device is a commercially available silicone rubber with a geometric cut-out in its center. Hydrogel components are polymerized to fill the cut-out. During polymerization, biological hydrogels, such as fibrin or collagen, naturally adhere to the interior walls of the cut-out. Using the SCyUS, the silicone strip is uniaxially stretched, transferring controlled strains to the embedded 3D hydrogel[41].

This system allows for a unique combination of features and advantages compared to other existing methods. First, the system allows uniaxial stretching of thick 3D soft hydrogels (> 100 µm thick, < 1 kPa stiffness) from their periphery, with *Z*-homogenous deformation throughout the

hydrogel. These hydrogels are too soft to be gripped and stretched by conventional tensile techniques. Second, the stretching device can be easily replicated in other labs since 3D printing is readily available to researchers and the electronics used in the design are low-cost. Third, and perhaps the most attractive feature, the geometry and the size of the cut-out in the silicone strip can be easily manipulated, allowing for tunable strain gradients and boundary conditions as well as the use of a variety of sample volumes, down to a few microliters.

The presented protocol consists of molding fibrin gel into ~2 mm diameter disks in 0.5 mm thick silicone rubber strips proceeded by uniaxial stretch under live confocal microscopy. The following discusses in detail the experimental procedures for measuring and analyzing the strains acting on the geometric cut-out, the internal strains developed in the hydrogel, as well as resulting fiber alignment after various stretch manipulations. Finally, the possibility of embedding cells in the hydrogel and exposing them to controlled external stretch is discussed.

PROTOCOL:

1. Solution preparation (to be performed in advance)

1.1. Fibrinogen labeling

NOTE: The labeling step is required only if analyzing the deformation of the fibrin gel is desired. For cellular experiments, it is possible to use an unlabeled gel.

1.1.1. Add 38 μL of 10 mg/mL succinimidyl ester fluorescent dye (dissolved in DMSO) to 1.5 mL of 15 mg/mL fibrinogen solution (molar ratio of 5:1) in a 50 mL centrifuge tube and place on a shaker for 1 hour at room temperature. Afterwards, place the tube in the centrifuge for 3 minutes at 800 x *g* (room temperature).

1.1.2. Filter the supernatant from the previous step through a desalting column packed with dextran gel resin (**Table of Materials**) to separate the unreacted dye,[42] by following these steps.

1.1.2.1. Pre-wash the column with 25 mL of fibrinogen buffer.

1.1.2.2. Slowly inject the labeled-fibrinogen from step 1.1.1 into the column, making sure that there are no bubbles entering the filter. Discard the first ~0.3 mL of eluted solution (4-6 drops of faint colored liquid). Then collect the following 1.0-1.5 mL of purified solution (follow manufacturer's protocol for more specific details).

1.1.2.3. Finish the filtration process by sterilizing the resulting purified solution using a syringe-driven filter (0.22-0.45 μm).

1.1.2.4. To clean and recycle the column, wash with 20 mL of fibrinogen buffer, and then store in 25 mL of 20% ethanol.

1.2. After elution, divide the resulting purified labeled-fibrinogen into small aliquots of ~7-50 μL, depending on the desired number of stretched gels. For each stretched 2 mm diameter circle gel, prepare about 3.5 μL of fibrinogen (2.5 μL will be used per gel + 1 μL for pipetting errors).

1.2.1. Store the aliquots in a -20 °C freezer. They can be used up to about one year (it is not recommended to thaw and freeze again).

1.2.2. For the remainder of this protocol, keep approximately 7 μL of the purified labeled fibrinogen in the refrigerator (4 °C) until step 4. This volume is intended for the creation of two stretched gels (2.5 μL is needed per gel, and an extra volume of 1 μL is used to account for errors in sample preparation).

NOTE: This filtering procedure typically dilutes the initial 15 mg/mL fibrinogen solution to a final concentration of about 10 mg/mL. The dilution factor depends on the initial volume and concentration of fibrinogen, as specified in the manufacturer's protocol.

1.3. Prepare 7 μL of thrombin solution (dilute using thrombin buffer to 2 units/mL, **Table of Materials**) and keep in the refrigerator (4 °C) until step 4. This volume is intended to fill the cut-outs of two stretched gels.

NOTE: In order to perform internal strain analysis, 1 μm diameter fluorescent spherical beads (purchased as a suspension [2% solids] in water plus 2 mM NaN_3) should be added to the thrombin solution (a ratio of 1:25 v/v % of bead:thrombin is recommended for a 40x objective). Beads should be included only when internal strain measurements are desired, either in the presence or absence of cells.

2. Silicone strip preparation

2.1. Retrieve the 0.5 mm thick silicone rubber and cut it into 15 x 80 mm^2 strips with a 2 mm diameter hole in the center of the strip (**Figure 1**). If possible, use a programmable laser cutter for high precision. If programmable machinery is not available, scissors are sufficient for cutting the strip outline and a small hole-punch is adequate for the center cut-out.

NOTE: Commercial silicone rubber is usually purchased with plastic wrap on both sides. Keep original plastic covering on both sides of the silicone if possible. If reusing silicone strips from a previous experiment, treat them with trypsin for 0.5 hour, soak in 0.2 M NaOH for 0.5 hour, and then soak in 70% ethanol for 1 hour. Let them dry before use.

2.2. Prepare sealing film (hydrophobic) layers with dimensions of at least 20 × 30 mm^2, so they are wider than the silicone strip and thus allowing for a seal to form over the entire geometric cut-out.

2.3. Wash a 10 cm dish with 70% ethanol, and then wipe and dry with non-linting delicate task wipes (for both sterile and non-sterile experiments). This step is important since it allows the

sealing film layers to better stick to the plate and restrict sample's movement during the preparation process.

2.4. Place the sealing film layers in the washed 10 cm dish so there is enough space to place two strips in each dish side-by-side (**Figure 2A**).

2.4.1. Remove the plastic wrap from one side of the silicone strip and place the exposed side on the sealing film layer so the cut-out is surrounded entirely by the sealing film layer (**Figure 2B**). Then, press gently on the silicone against the sealing film layer in order to seal the area surrounding the cut-out, using clean gloved fingers.

NOTE: Ensure there are no air-pockets between the silicone and the sealing film, especially around the cut-out. Do this by examining the bottom-side of the dish (**Figure 2C**).

[Place **Figure 1** here]
[Place **Figure 2** here]

3. Preparing thrombin with cells

NOTE: Perform this step only if embedding cells in the hydrogel is desired, and under sterile conditions in a biological hood (**See Table of Materials**).

3.1. Sterilization: the day prior to the cellular experiment, place the silicone strips & sealing film layers in 70% ethanol overnight and then perform UV sterilization for 30 minutes on each side (if the 10 cm dishes are not already sterile, they should also be sterilized under UV light for 30 minutes after a 70% ethanol wash). The UV system utilized in the protocol is the one built into the biological hood.

NOTE: Alternatively, an autoclave sterilization cycle (140 °C) can be performed on the silicone strips since they are resistant to up to 260 °C.

3.2. Perform a cell count to determine cell concentration, and then centrifuge and re-suspend the cell pellet with 7 μL of thrombin (2 units/mL) in a 1.5 mL centrifuge tube. We recommend a cell concentration of 800 cells/μL of thrombin. Keep the cells chilled until use (do not exceed more than half an hour to avoid damaging the cells).

4. Polymerization of fibrin gels

4.1. Retrieve the 2 Unit/mL thrombin & 10 mg/mL labeled-fibrinogen solutions from the refrigerator (prepared in step 1) and place them on ice where they will be accessible.

NOTE: Solutions are kept cold prior to the mixing process in order to slow down the polymerization reaction kinetics. This allows for more homogenous mixing of the proteins.

4.2. With the dish(es) set up (step 2), extract 2.5 μL of labeled-fibrinogen and pipette it uniformly into the silicone cut-out (with the sealing film layer attached to its bottom side) so that the entire circumference of the cut-out is in contact with fibrinogen. Be careful not to allow any air-pockets or bubbles to form anywhere in the solution, paying particular attention to the bottom edges of the cut-out (the interface between the sealing film layer and silicone).

4.3. Immediately take 2.5 μL of thrombin (with or without cells/beads) and pipette it directly into the fibrinogen solution in the cut-out (reaching final volume of 5 μL fibrin). Then quickly mix the two solutions by carefully pipetting up and down ~10 times. During the mixing process, move the tip around the entire volume to create as homogenous a solution as possible.

4.4. Add a very small amount of Phosphate Buffer Saline (PBS) [alternatively cell medium for cell experiments, **Table of Materials**] along the edge of each dish so the hydrogel does not dry out during the polymerization process. Ensure there is no contact between the PBS/cell medium and the samples as this will damage the sample.

4.5. Cover the dish(es) and place them in the incubator at 37 °C for 30 minutes.

NOTE: The required incubation time is dependent on the volume of the gel. If larger volumes are used, the incubation time should increase.

4.6. Remove the dish(es) from the incubator and add PBS/cell medium to the dish, submerging the entire gel-silicone construct.

4.7. Carefully lift the sample constructs one at a time from the dish making sure the sealing film layer remains adhered to the strip. Slowly detach the sealing film layer from the silicone by gently pealing from one end of the silicone to the other (**Figure 3**). Avoid pulling from areas close to the cut-out where stress concentrations may exist (this is mainly important for non-circular geometries). Avoid any contact with the cut-out as it will damage the sample.

4.8. Place the strip back into the dish with PBS/cell medium such that the strip is floating in the dish. Then take the dish(es) to a standard cell-culture microscope to qualitatively assess the condition of each sample. Gels must be uniform, continuous throughout the cut-out, and no bubbles should be present. Using **Figure 4** as a guide, select the best samples for further analysis.

[Place **Figure 3** here]
[Place **Figure 4** here]

5. Sample loading on the SCyUS device

5.1. Fill the bath with PBS/cell medium (**Figure 5**) and place the silicone strip carrying the sample gel across the top so the ends are sitting on each side of the bath. The bath is meant to avoid any drying of the gel. Place and tighten the clamps (purple) along with the fabric strips (green) so that all pieces are connected to form one straight strip with the cut-out in the center (**Figure 5**).

5.2. Retrieve the SCyUS device and attach the aluminum liquid well and 22 mm x 40 mm rectangular glass coverslip (No. 1 or 1.5) (**Figure 6Aiii**). Attach the cover slip to the bottom of the well using sealing material (e.g., vacuum grease) so that the well can be filled with liquid without leakage.

5.2.1. Fill the well with ~1-2 mL of PBS/cell medium and place the strip + fabric + gel construct (**Figure 6B**) into the device. Clamp the fabric strip (**2**) into the bracket (**1**) so that the cut-out + gel (**5**) is in the center as shown, then carefully place the pin-down insert (**4**) into the device and lock it in place.

5.2.2. Next, insert the other fabric side to the spindle (without attaching the servomotor) and lock it into the spindle (**Figure 6C**).

5.3. Insert the SCyUS device with the attached sample into the stage of the microscope (**Figure 6C**). Connect the microcontroller (**Table of Materials**) to the computer via a USB cable and connect the servomotor to the microcontroller. Open the SCyUS control module on the computer. The sample is now ready for imaging to check the adequacy of the gel's thickness and fiber homogeneity under the confocal microscope.

[Place **Figure 5** here]
[Place **Figure 6** here]

6. Ensure adequate gel for sampling

6.1. Using the confocal microscope (**Table of Materials**) take a low-magnification (10×), low-resolution (~1.4 μm x 1.4 μm pixel size) confocal Z-stack (≤10 Z-slices with a step size of approximately 10 μm is sufficient) tile image of the entire gel using lasers of 488/543/561 to examine homogeneity and adhesion to the circumference of the geometric cut-out throughout the thickness of the silicone (**Figure 7A-B**). Use this *Z*-stack image as a map for the following steps.

6.2. Using low-resolution live imaging, scan the gel and determine the lowest *Z*-position where full adhesion to the inner walls of the cut-out is apparent with no tears or bubbles and note the *Z*-location of the microscope (Z_ℓ). To determine full adhesion of the gel to the silicone throughout its circumference, scan the interface of the fluorescent label of the gel and the silicone strip (dark background) under the microscope (**Figure 7C**).

6.3. Move up in the *Z*-direction until there is no longer continuity in the gel and note the *Z*-position (Z_u):

6.4. Subtract the upper limit (Z_u) of the *Z*-direction from the lower limit (Z_ℓ). This is the reference thickness of the sample (Z_o):

$$Z_o = Z_u - Z_\ell \qquad (1)$$

If $Z_o \geq 100$ μm then the gel is considered satisfactory for analysis. Note that the thickness of the silicone cut-out is about 500 μm, but gel polymerization in the cut-out typically results in a smaller gel thickness. 100 μm is the minimum recommended thickness to ensure a stable stretching process, without tears or detachment of the gel from the silicone cut-out.

NOTE: At different XY locations, the thickness of the gel can vary. This section of the protocol measures the minimum thickness of the gel, allowing us to determine the gel quality and indicate if it is sufficient for stretching. Additionally, finding the center of the gel provides a reference point to return to post-stretching, whether static or dynamic.

[Place **Figure 7** here]

7. SCyUS operation, stretching & imaging

7.1. Now that the sample has been determined to be of satisfactory quality and is set on the SCyUS device properly, determine the pre-stretched position of the sample. This is achieved by using *live* imaging under the confocal microscope (similar to step 6.2).

7.1.1. Make sure the servomotor is at its zero position by clicking the **Go To Zero Servo Pos** button (Click on **Figure 8A** and ensure that **Figure 8B** displays zero) and attach it to the stretching device as seen in **Figure 6C**.

NOTE: Do this step slowly and carefully as not to put any excess tension on the sample.

7.1.2. While imaging the sample, move the motor one degree (**Figure 8C**) at a time in the clockwise direction by clicking the **+1** button until the right side of the cut-out is observed to move. Then, reverse the movement (**Figure 8D**) back to the penultimate step position by clicking on the **-1** button. This verifies that the sample is under minimal tension. Click on the **Set Min Servo Position** button (**Figure 8E**) to set the reference position. It is possible to return to the reference position at any time by clicking the **Go To Min Servo Position** button (**Figure 8F**).

NOTE: It is recommended to use a high-magnification objective (≥40×) for this step to minimize error.

7.1.3. Capture a high-magnification (40×), high-resolution (~0.2 μm × 0.2 μm pixel size), single Z-slice tile image of the entire gel area. This will be used as the reference image for post-processing analysis. It is recommended to capture a single *Z*-slice image in the middle of the gel thickness (by using Z_o from **Eq. 1**), this will allow for the return to approximately the same *Z*-position after stretching. Also, take into consideration that high-resolution tile images of the entire gel area take considerable time (~20-30 min).

7.1.4. Now the sample is ready for static stretching. Adjust the servomotor to the desired stretch magnitude by advancing one degree (**Figure 8C**) at a time in the GUI (perform this slowly, about 1 degree/second).

7.2. At each stretch magnitude where analysis is desired, capture a single Z-slice high-resolution tile image of the entire gel area for post-processing analysis. Similar to step 6.2, verify that the gel has not detached from the silicone throughout its circumference by scanning the interface between the gel (red) and the silicone (dark background), looking for changes in the adhesion from the previous stretch magnitude.

NOTE: During the activation of the motor, use *live* imaging to follow the gel location in *X*-*Y* (with low-resolution, low-magnification settings). The gel experiences a *Z*-Poisson effect where the bottom of the gel rises, therefore the *Z*-position of the microscope should also be adjusted to the approximate center of the gel thickness for every stretch magnitude. This can be achieved by recalculating Z_o (**Eq. 1**) for each stretch magnitude. Since stretch in the *Z*-direction is relatively homogenous, it is not critical to find the exact center depth of the gel.

[Place **Figure 8** here]

8. Post-processing external strain measurements

8.1. To measure the effective strains of the cut-out boundaries, measure the edge-to-edge lengths in the stretch direction (*X*-axis) at the center of the *Y*-axis (**Figure 9A**).

8.1.1. Upload the pre-stretch image to the image processing software (ImageJ FIJI[43]) and measure the largest-edge-to-edge distance which is defined as the axial length of the hole (ℓ_o) at the center.

8.1.2. Define the largest distance from top to bottom as the perpendicular distance (d_o).

8.1.3. Repeat this process for all stretch interval images and calculate the axial (ℓ) and perpendicular (d) distances of the cut-out periphery (**Figure 9A**, bottom) and then perform the following calculations to find the strains of the cut-out edges:

$$\varepsilon_{xx}(hole) = \frac{\ell - \ell_o}{\ell_o} \quad (2)$$

$$\varepsilon_{yy}(hole) = \frac{d - d_o}{d_o} \quad (3)$$

[Place **Figure 9** here]

9. Fiber orientation analysis

9.1. Use quantification of fiber alignment to characterize the structural response of the fibrous gel to increasing magnitudes of stretch. Upload high-resolution images to ImageJ FIJI software (NIH)[43] and then analyze using the OrientationJ (EPFL)[44] module (Settings: Gaussian gradient, and 3-pixel window, **Figure 10**).

9.1.1. Calculate the 2D Nematic Order Parameter (NOP) of the orientation histogram as: [45]

$$NOP = 2\langle(cos\,\theta)^2\rangle - 1 \qquad (4)$$

NOTE: A value of NOP = 1 indicates perfect alignment along the axial direction (angle zero) and NOP = 0 indicates isotropy. The orientation angle, θ, is the fiber angle in relation to the strain axis (x-axis) obtained through image analysis and precisely defined in the OrientationJ documentation.[44]

[Place **Figure 10** here]

10. Manual internal gel strain analysis

10.1. While performing live high-magnification imaging of a hydrogel with embedded beads, manually locate a region of interest (ROI) with easily recognizable features (e.g., aggregates of beads), in order to return to the same location after each stretch magnitude.

NOTE: Compression in the Z-direction (Poisson effect) can lead to an increase in bead density as stretch increases, therefore we suggest choosing bead aggregates large enough, so they are clearly identifiable. This protocol calls for the analysis of the central region of the fibrin gel, though any region can be chosen.

10.2. In the pre-stretch position (step 6), capture a high-resolution *Z*-stack image of the selected ROI. After each desired stretch interval, return to the same ROI and repeat the image capture process.

10.3. Take the images and import them into ImageJ. In the ROI, record the *X*-*Y* pixel location of each visible bead aggregate. Transfer the recorded data to a spreadsheet.

10.4. Measure the distances between every pair of aggregates and compare them to the distances of the same pairs in the reference image, allowing calculation of strains in the *X* and *Y* directions.

NOTE: If a continuous real-time movie is recorded while the gel is stretched (instead of static image capture), an automatic analysis of strains can be performed with digital image or volume correlations (DIC/DVC) methods, as previously demonstrated[46,47]. However, it should be noted that automatic DIC/DVC analysis is challenging in this setting, as the *Z*-stack is not only moving in the *X*-*Y* plane but also in the *Z*-direction due to the Poisson effect (compression), accounting for considerable drifts during the recorded movie.

REPRESENTATIVE RESULTS:

Representative data from static stretch of increasing magnitudes applied to the silicone strip carrying a 3D fibrin hydrogel, embedded with 1 μm fluorescent beads, is shown in **Figure 9**. The analysis demonstrates the effect of silicone stretch on geometric changes of the cut-out as well as the developed strains within the gel. *Z*-stack images of the entire gel are used to evaluate the deformation of the original circle shaped cut-out to the elliptical geometry (**Figure 9A**). These

images are used to calculate ε_{xx}(hole) (**Equation 2**). Zooming in and manually tracking several bead aggregates (**Figure 9B**) during gel stretching, allows for the calculation of local gel strains at the center, in the axial $\varepsilon_{xx}(gel)$ and perpendicular $\varepsilon_{yy}(gel)$ directions (**Figure 9C,D**). The axial strains propagate relatively linearly from the silicone cut-out edge to the center of the gel and are larger than the compressive perpendicular strains (**Figure 9D**).

High-magnification images of the fluorescently labeled gel allows for observation and quantification of fiber alignment, induced by the silicone stretch. **Figure 11** shows representative zoom-in images of a typical un-stretched and relatively isotropic hydrogel (**Figure 11A**) and a hydrogel under high 80% cut-out strain depicting highly aligned fibers in the stretch direction (**Figure 11B**). Analysis of fiber reorientation using ImageJ revealed approximately linear dependence between fiber alignment (NOP) and the external strain on the cut-out (ε_{hole}) up to strains of 40%, with moderate saturation at strains above 40% (**Figure 11D**). A detailed analysis of fiber alignment in different *Z*-slices is shown in **Figure 12**. Here, histograms of fiber alignment are calculated for each *Z*-slice (**Figure 12A**), as well as their corresponding NOP (**Figure 12B**)**,** and the averaged NOP over all *Z*-slices for each external strain magnitude of the cut-out (**Figure 12C**). As ε_{hole} increases, fiber alignment increases, following an overall non-linear curve as shown in **Figure 12C.** Note that the gel contracts along the *Z*-axis due to the Poisson effect, represented by the shorter lines at higher strains in **Figure 12B**.

Since it has proven difficult to perform in-depth analysis of the internal strains in the entire gel, we provide here preliminary results of finite element (FE) simulations performed on 2D continuous material given the mechanical properties of fibrin (**Figure 13**). The external strain of the cut-out is ~40% and the color-map represents the stretch-induced strain field. The color-map ranges from 38%-42%, indicating that gel strains are relatively homogenous throughout the circular gel area. We note that if other gel geometries are used, gradients in strain may arise, and this is a topic for future studies.

In order to demonstrate that embedded fibrin gels can sustain adhesion to the silicone strip at high strains (0 to +30%) and frequencies (up to 1 Hz), we ran preliminary tests (protocol for this test is not included in this work) showing no detachments of the gels from the inner walls of the cut-out. Three gels were tested, gel 1 for a total duration of ~87 minutes, gel 2 for 60 minutes & gel 3 for 30 min total (**Table 1**). In all three of these cases fibrin hydrogels maintained their adhesion to the silicone.

FIGURE AND TABLE LEGENDS:

Figure 1: **Hydrogel straining approach (A**) 15 × 80 mm^2 silicone strip with a 2 *mm* diameter cut-out in the center of the strip (**B**) A silicone strip with a circular cut-out with embedded fibrin gel. For illustrative purposes, the cut-out in the silicone is larger than in the actual experiments (**C**) Schematic of the stretching approach with the silicone strip (orange), circular gel (cut-out in the middle), and fabric extenders (green) that connect the silicone to the stretching device. Enlarged area of the gel indicates the deformation of the gel, in response to uniaxial stretching of the silicone. For simplicity, the compression along the thickness of the gel (*Z*-axis) is not shown in the illustration. Figures **1B** & **1C** have been adapted from Roitblat Riba et al.[41]

Figure 2: **Example of proper placement of a silicone strip on a sealing film layer prior to gel polymerization (A**) Placement of two sealing film layers in a 10 *cm* dish (**B**) Placement of silicone strips on the sealing film layers (**C**) Bottom-view of the dish, displaying the air-seal between the silicone and the sealing film layer. **Left**: Proper seal of the sealing film layer to the silicone strip around the cut-out without air-pockets. **Right**: Improper seal of the sealing film layer to the silicone strip cut-out with air-pockets around the edge of the cut-out. This will lead to leaking of the hydrogel components underneath the silicone. Red arrow points to an area where an air-pocket was formed.

Figure 3: **Proper removal of the sealing film layer from the bottom of the silicone strip.** The removal process should be done slowly so the hydrogel will not tear or break its adhesion with the inner walls of the cut-out. The white arrow shows the direction of removal.

Figure 4: **Microscopic observation of fibrin gels in the silicone cut-out (A**) Two examples of a properly polymerized fibrin gel. Notice the relative homogeneity of the gel and the full adhesion to the edges of the cut-out (**B**) Two examples of sample polymerization failure. **Top**: Notice the many bubbles and the aggregates formed on the bottom left side. **Bottom**: Notice the tearing of the gel from the cut-out edges and the aggregates in the bottom left region of the cut-out. Scale bar = 300 μm

Figure 5: (**A**) Jig containing a PBS bath (3D printed) (**B**) Strip placement on the jig to ensure proper in-line attachment of brackets (in purple) and preventing drying of the gel. This figure has been modified with permission from Roitblat Riba et al.[41]

Figure 6: **SCyUS stretching device (A**) Several views of a CAD model of the main parts of the SCyUS: spindle connected to the servo (blue), static anchor (red), insert that pins the silicone strip down (purple) and fixers that prevent the insert from rising up (yellow-green). A top view of the system (**Ai**), a cut view of the system (**Aii**) showing the path of the strip (orange line), and a bottom view (**Aiii**) of the aluminum liquid well with a glass coverslip. The liquid well can be moved up and down with the turn of a screw fitted into the major threading. The upward movement of the aluminum well is limited by the purple insert's side wings, as shown by the white arrows (**B**) The actual system: (**1**) static anchor (**2**) green non-stretchable fabric (**3**) screw for aluminum liquid well height control (**4**) red pin-down insert (**5**) a silicone strip with a circular cut-out (**6**) blue connecting clamps (**C**) The stretching system placed on a confocal microscope. The servomotor and the spindle are shown with arrows. This figure has been modified with permission from Roitblat Riba et al.[41]

Figure 7: **Gel homogeneity.** Tile images were captured and stitched using the confocal microscope software (See **Table of Materials**) (**A**) A single stitched tile *Z*-slice image of a fibrin gel sample with relatively inhomogeneous fiber density due to improper thrombin and fibrinogen mixing pre-polymerization. This gel will not provide a reliable analysis (**B**) A single stitched tile *Z*-slice image of a fibrin gel sample with relatively homogenous fiber density. This is an acceptable gel for stretching experiments. Scale bar for images A & B is 200 *μm* (**C**) Zoom in of the interface

between the fluorescently labeled gel (red) and the silicone (black background). Scale bar = 100 μm.

Figure 8: **GUI for the SCyUS control module (A**) Position of the motor in degrees. The value ranges from -90° to 90° (**B**) 'Set Minimum Servo Position'. This button allows for a pre-set minimum position, for setting a new reference position that is different from the Zero Servo Position (**C**) 'Plus 1°' button moves the servo motor one-degree clockwise (**D**) 'Minus 1°' button moves the servo motor one-degree counter-clockwise (**E**) 'Go to zero position' button sets the servomotor position to 0° ([**A**] will be set to zero) (**F**) 'Go to minimum servo position' button moves the servomotor to the user defined 'Min' position.

Figure 9: **Gel strains due to external stretching of the silicone strip (A**) *X-Y* cross-section of an un-stretched fibrin gel (top), and after application of ε_{hole} = 64% strain along the x direction (bottom). The gel is embedded with fluorescent beads. The relevant lengths of *d* and *l* used for calculation of ε_{hole} are indicated in the images (**B**) Zoom-in images of the dashed square area marked in **A** (**C**) Illustration of the strain types considered in this study: ε_{hole} is the axial strain of the cut-out at its maximum diameter, and ε_{gel} is the axial strain in the center of the gel (as measured by the bead aggregate locations) (**D**) A linear relationship was found between ε_{hole} and ε_{gel} in both *xx* direction (red line) and *yy* direction (green line). This figure has been adapted with permission from Roitblat Riba et al.[41]

Figure 10: **Fiber orientation analysis using FIJI ImageJ software (A**) Main Menu of ImageJ with an arrow indicating the location of the 'Plugins' pulldown menu where 'OrientationJ' can be found. Under the extended menu of 'OrientationJ', click on the 'OrientationJ Distribution' option (**B**) OrientationJ's Distribution module. Set 'Local window σ' to 3 pixels and 'Gradient' to 'Gaussian'. Then press the 'Run' button (red arrow).

Figure 11: Gel fiber alignment in response to external stretch. Images taken at the center of a fluorescently-labeled gel while (**A**) unstretched and (**B**) after the application of ε_{hole}= 80% (**C**) Averaged histograms of fiber orientations under increasing ε_{hole} [%] strains. Grey error bars indicate differences between 40 slices in the z-stack assessed for each tested strain (**D**) Averaged Nematic Order Parameter (NOP) as a function of ε_{hole} for three different gel samples (including "Gel 1" that is analyzed in **Figure 11A-C**). Error bars indicate differences between slices in the *Z*-stack of each stretch magnitude. This figure has been adapted with permission from Roitblat Riba et al.[41]

Figure 12: Analysis of fiber orientation using the OrientationJ[44] tool (ImageJ software)[43] (**A**) 3D histograms of fiber orientation for different *Z*-slices. Shown are examples of two histograms calculated for stretched (ε_{hole} = 17.6%, top) and un-stretched (bottom) gels. The histogram is normalized such that the area under the curve is equal to 1 (**B**) Resulting NOP versus *Z*-depth; the graph shows the calculations of NOP of each histogram as a function of *Z*-depth (**C**) Mean NOP as a function of ε_{hole}. Error bars represent the standard deviation of NOP for all the *Z*-slices in an individual stretch magnitude at the same XY point in the same gel.

Figure 13: 2D finite elements (FE) simulation of a stretched gel. Gel is stretched ($\varepsilon_{hole} \approx 40\%$) by a silicone carrier. Strain field is presented with values of maximum principal strain where minor gradients are observed. The circle represented by the dotted line is the pre-strained geometry of the hole, the original length (l_o) is the center length along the x-axis before stretch is applied, and the stretched length (l) is the center length along the x-axis after stretch is applied.

Table 1: **Representative results of dynamic stretch proof of concept.** Three gels were embedded in silicone strips and stretched dynamically (1 Hz) for various durations. Strains ranged from zero to various magnitudes above 30%. All three gels of these successfully sustained their adhesion to the inner walls of the circular cut-out of the silicone strip.

DISCUSSION:

The method and protocol presented herein are largely based on our previous study by Roitblat Riba et al.[41] We include here the full computer-aided design (CAD), Python and microcontroller codes of the *SCyUS* device.

The major advantages of the presented method over existing approaches include the possibility to strain very soft 3D hydrogels (Elastic Modulus of ~100 Pa) from their circumference, and under *live* confocal imaging. Other methods are usually limited in their ability to apply strain fields in the *Z*-axis and are unable to provide in situ high-magnification microscopy images while stretching, mostly due to working distance limitations from the sample to the objective lens. Most available systems are based on 2D substrate-stretching, which are limited in mimicking physiological tissue environments.

Limitations of the system include potential inconsistent homogeneity of fiber density of the gel post-polymerization (**Figure 7A**), especially when large gel volumes or complex geometries are used. Such non-homogeneities can lead to non-uniform strains and fiber alignment in the gel. Moreover, optical restrictions at relatively deep *Z*-sections (>30 μm) may give rise to errors in analysis of fiber orientation.

Critical steps in the 3D stretching protocol include the following (i) Ensure that sample gels have achieved complete adhesion to the inner walls of the geometric cut-out within the silicone, without bubbles or tears, especially along the *Z*-direction. Complete adhesion and continuity of the sample with a thickness of at least 100 μm (**Eq. 1**) is crucial to reliably stretch the sample to a desired strain (*ii)* Properly attach the sample to the *SCyUS* device prior to stretching. It is necessary to attach the silicone strip to the brackets and non-elastic fabric length extenders using the 3D printed jig (**Figure 5A**) and to validate that all pieces are attached in-line, ensuring that strain is induced in the gel symmetrically. This also applies to the correct loading of the device's spindle (**Figure 6B-C**) (*iii)* Carefully capture the reference (pre-stretch) position of the sample. If the reference image is taken while the sample is already under tension (e.g., due to the attachment of the servomotor prior to this step), all strain measurements will be inaccurate.

Potential future applications and modifications of the presented protocol include the following. (i) A cyclic stretch regime can be applied to the cell embedded hydrogels. As dynamic movement

of the motor is encoded by the microcontroller software, any cyclic profile can be programmed, constrained only by the resolution and the rotation speed of the motor employed in the system (more details available in Roitblat Riba et al.[41]). In this work, we demonstrated that fibrin gel can sustain adhesion under dynamic stretch (**Table 1**). Though further testing is necessary, the application of cyclic loading would provide insights into the dynamic response of the hydrogel and embedded cells.

(ii) The geometry and volume of the silicone cut-out can be modified. In the current protocol, we focused only on gels in a circular geometry. Under such conditions, internal strains are relatively homogeneous throughout the gel, as predicted by our FE simulations (**Figure 13**). However, if other gel geometries will be considered by modifying the cut-out section of the silicone, gradients will emerge. For example, a 'diamond' shaped cut-out could potentially lead to a gradient in the gel strains due to a gradual change in the initial length of the cut-out along the direction of stretch. This method of gel strain control is especially appealing, as different shaped cut-outs are relatively trivial to manufacture. Additionally, the thickness and the area of the silicone cut-out could be easily altered allowing for adjustments in gel volumes, from miniature volumes of a few microliters to larger volumes associated with *mm-cm* scale gel sizes. Moreover, it is possible to include several cut-outs in the same silicone strip, allowing for stretching of several gels simultaneously.

(iii) Cells can be embedded in the hydrogel. There are a few challenges that should be taken into consideration when embedding cells in the stretched hydrogels. Most cells embedded in 3D hydrogels apply considerable traction forces on the matrix, as well as degrading the matrix over time. This can result in global contraction and digestion of the gel, which can lead to disconnection of the gel from the silicone cut-out inner wall at prolonged times of incubation. A possible way to cope with this situation is to use low cell concentrations and limiting the time of cellular experiments to an interval that gel contraction and degradation are minimal. We have previously demonstrated the possibility of culturing fibroblast cells in the fibrin gel under static stretch of 10%, over a period of 5 hours, without any evidence of gel tearing or disconnection from the silicone cut-out[41].

(iv) This setup should also be tested with other types of hydrogels, in particular synthetic ones such as polyacrylamide (PAA) or polyethylene glycol (PEG)-based hydrogels, which are commonly used for cell culture. The natural adhesion of these hydrogels to the silicone cut-out should be examined, and if found to be insufficient for gel stretching, then techniques to encourage adhesion should be used. The use of biological glues[48,49] or chemical treatments[50,51,52] to the cut-out surface should be considered.

ACKNOWLEDGMENTS:

Some figures included here have been adapted by permission from the Copyright Clearance Center: Springer Nature, *Annals of Biomedical Engineering*. Straining 3D hydrogels with uniform z-axis strains while enabling live microscopy imaging, A. Roitblat Riba, S. Natan, A. Kolel, H. Rushkin, O. Tchaicheeyan, A. Lesman, Copyright© (2019).

https://doi.org/10.1007/s10439-019-02426-7

DISCLOSURES:

The authors have nothing to disclose.

REFERENCES:

[1]Bleuel, J., Zaucke, V., Bruggemann G. P., Niehoff, A. Effects of cyclic tensile strain on chondrocyte metabolism: a systematic review. *PLoS ONE*. **10**, e0119816 (2015).

[2]Pennisi, C. P., Olesen, C. G., de Zee, M., Rasmussen J., and Zachar, V. Uniaxial cyclic strain drives assembly and differentiation of skeletal myocytes. *Tissue Engineering Part A*. **17**, 2543–2550 (2011).

[3]Grodzinsky, A. J., Levenston, M. E., Jin, M., Frank E. H. Cartilage Tissue Remodeling in Response to Mechanical Forces. *Annual Review of Biomedical Engineering*. **2**(1), 691-713 (2000).

[4]Munster, S. et al. Strain history dependence of the nonlinear stress response of fibrin and collagen networks. *Proceedings of the National Academy of Sciences of the USA*. **110**, 12197–12202 (2013).

[5]Vader, D., Kabla, A., Weitz, D., Mahadevan, L. Strain-induced alignment in collagen gels. *PLoS ONE*. **4**, 5902 (2009).

[6]Badylak, S. F. The extracellular matrix as a scaffold for tissue reconstruction. *Seminars in Cell & Developmental Biology*. **13** (5), 377-383 (2002).

[7]Natan, S., Koren, Y., Shelah, O., Goren, S., Lesman, A. *Molecular Biology of the Cell*. **31** (14), 1474-1485 (2020).

[8]Ban, E. et al. Mechanisms of Plastic Deformation in Collagen Networks Induced by Cellular Forces. *Biophysical Journal*. **114** (2), 450-461 (2018).

[9]Kim, J. et al. Stress-induced plasticity of dynamic collagen networks. *Nature Communications.* **8**, 842 (2017).

[10]Storm, C., Pastore, J. J., MacKintosh, F. C., Lubensky, T. C., Janmey, P. A. Nonlinear elasticity in biological gels. *Nature.* **435**, 191–194 (2005).

[11]Wen, Q., Basu, A., Janmey, P. A., Yodh, A. G. Non-affine deformations in polymer hydrogels. *Soft Matter.* **8**, 8039–8049 (2012).

[12]Muiznieks, L. D., Keeley, F. W. Molecular assembly and mechanical properties of the extracellular matrix: A fibrous protein perspective. *Biochimica et Biophysica Acta.* **1832,** 866–875 (2012).

[13]Brown, A. E. X., Litvinov, R. I., Discher, D. E., Purohit, P. K., Weisel, J. W. Multiscale mechanics of fibrin polymer: gel stretching with protein unfolding and loss of water. *Science.* **325**, 741–744 (2009).

[14]Carroll, S. F., Buckley, C. T., Kelly, D. J. Cyclic tensile strain can play a role in directing both intramembranous and endochondral ossification of mesenchymal stem cells. *Frontiers in Bioengineering and Biotechnology*. **5**, 73 (2017).

[15]Livne, A., Bouchbinder, E., Geiger, B. Cell reorientation under cyclic stretching. *Nature Communications.* **5**, 3938 (2014).

[16]Wang, L. et al. Patterning cellular alignment through stretching hydrogels with programmable strain gradients. *ACS Applied Materials & Interfaces.* **7**, 15088–15097 (2015).

[17]Xu, G. K., Feng, X. Q., Gao, H. Orientations of Cells on Compliant Substrates under Biaxial Stretches: A Theoretical Study. *Biophysical Journal*. **114** (3), 701-710 (2017).

[18]Chagnon-Lessard, S., Jean-Ruel, H., Godin, M., Pelling, A. E. Cellular orientation is guided by strain gradients. *Integrative Biology (United Kingdom)*. **9** (7), 607-618 (2013).
[19]Lu, J. et al. Cell orientation gradients on an inverse opal substrate. *ACS Applied Materials & Interfaces*. **7** (19), 10091-10095 (2015).
[20]Baker, B. M., Chen, C. S. Deconstructing the third dimension – how 3D culture microenvironments alter cellular cues. *Journal of Cell Science.* **125**, 3015-3024 (2012).
[21]Bono, N. et al. Unraveling the role of mechanical stimulation on smooth muscle cells: a comparative study between 2D and 3D models. *Biotechnology and Bioengineering.* **113**, 2254–2263 (2016).
[22]Pampaloni, F., Reynaud, E. G., Stelzer, E. H. K. The third dimension bridges the gap between cell culture and live tissue. *Nature Reviews Molecular Cell Biology*. **8**, 839–845 (2007).
[23]Riehl, B. D., Park, J. H., Kwon, I. K., Lim, J. Y. Mechanical stretching for tissue engineering: two-dimensional and three-dimensional constructs. *Tissue Engineering Part B: Reviews.* **18**, 288–300 (2012).
[24]Flexcell. Linear Tissue Train Culture Plate (2019).
[25] Flexcell. Tissue Train (2019).
[26]CellScale. MCT6 Stretcher (2019).
[27]STREX. STB-150 (2019).
[28] STREX. Stretch Chambers (2019).
[29]Kamble, H., Barton, M. J., Jun, M., Park, S., Nguyen, N. T. Cell stretching devices as research tools: engineering and biological considerations. *Lab on a Chip.* **16**, 3193– 3203 (2016).
[30]Weidenhamer, N. K., Tranquillo, R. T. Influence of cyclic mechanical stretch and tissue constraints on cellular and collagen alignment in fibroblast-derived cell sheets.
Tissue Engineering Part C: Methods. **19**, 386–395 (2013).
[31]Yung, Y. C., Vandenburgh, H., Mooney, D. J. Cellular strain assessment tool (CSAT): precision-controlled cyclic uniaxial tensile loading. *Journal of Biomechanics.* **42**, 178–182 (2009).
[32]Chen, K. et al. Role of boundary conditions in determining cell alignment in response to stretch. *Proceedings of the National Academy of Sciences of the USA.* **115**, 986–991 (2018).
[33]Heher, P. et al. A novel bioreactor for the generation of highly aligned 3D skeletal muscle-like constructs through orientation of fibrin via application of static strain. *Acta Biomaterialia*. **24**, 251–265 (2015).
[34]Foolen, J., Deshpande, V. S., Kanters, F. M. W., Baaijens, F. P. T. The influence of matrix integrity on stress-fiber remodeling in 3D. *Biomaterials.* 33, 7508–7518 (2012).
[35]Walker, M., Godin, M., Pelling, A. E. A vacuum-actuated microtissue stretcher for long-term exposure to oscillatory strain within a 3D matrix. *Biomedical Microdevices.* **20**, 43 (2018).
[36]Zhao, R. G., Boudou, T., Wang, W. G., Chen, C. S., Reich, D. H. Decoupling cell and matrix mechanics in engineered microtissues using magnetically actuated microcantilevers. *Advanced Materials.* **25**, 1699–1705 (2013).
[37]Li, Y. H. et al. Magnetically actuated cell-laden micro-scale hydrogels for probing strain-induced cell responses in three dimensions. *NPG Asia Materials*. **8**, e238 (2016).
[38]Li, Y. H. et al. An approach to quantifying 3D responses of cells to extreme strain. *Scientific Reports.* **6**, 19550 (2016).
[39]Humphrey, J. D. et al. A theoretically-motivated biaxial tissue culture system with intravital microscopy. *Biomechanics and Modeling in Mechanobiology*. **7**, 323–334 (2008).

747 [40]Niklason, L. E. et al. Enabling tools for engineering collagenous tissues integrating bioreactors,
748 intravital imaging, and biomechanical modeling. *Proceedings of the National Academy of Sciences*
749 *of the USA.* **107**, 3335–3339 (2010).
750 [41]Roitblat Riba, A. et al. Straining 3D hydrogels with uniform z-axis strains while enabling live
751 microscopy imaging. *Annals of Biomedical Engineering*. (2019).
752 [42]Gomez, D., Natan, S., Shokef, Y., Lesman, A. Mechanical interaction between cells facilitates
753 molecular transport. **3** (12), 1900192 *Advanced Biosystems* (2019).
754 https://doi.org/10.1002/adbi.201900192.
755 [43]Schindelin, J. et al. Fiji: an open- source platform for biological-image analysis. *Nature Methods.*
756 **9**, 676–682 (2012).
757 [44]EPFL Switzerland. OrientationJ plug in (2019).
758 [45]Goren, S., Koren, Y., Xu, X., Lesman, A. Elastic anisotropy governs the decay of cell-induced
759 displacements. *Biophysical Journal*. **118** (5), 1152-1164 (2019).
760 https://doi.org/10.1016/j.bpj.2019.12.033.
761 [46]Notbohm, J., Lesman, A., Tirrell, D. A., Ravichandran, G. Quantifying cell-induced matrix
762 deformation in three dimensions based on imaging matrix fibers. *Integrative Biology.* **7** (10),
763 1186-1195 (2015).
764 [47]Lesman, A., Notbohm, J., Tirrell, D. A., Ravichandran, G. Contractile forces regulate cell division
765 in three-dimensional environments. *Journal of Cell Biology.* **205** (2), 155-162 (2014).
766 [48]Cha, C. Y. et al. Tailoring Hydrogel Adhesion to Polydimethylsiloxane Substrates Using
767 Polysaccharide Glue. *Angewandte Chemie International Edition*. **52**, 6949-52 (2019).
768 [49]Wirthl D. et al. Instant tough bonding of hydrogels for soft machines and electronics. *Science*
769 *Advances*. **3** (2017).
770 [50]Juarez-Moreno, J. A., Avila-Ortega, A., Oliva, A. I., Aviles, F., Cauich-Rodriguez, J. V. Effect of
771 wettability and surface roughness on the adhesion properties of collagen on PDMS films treated
772 by capacitively coupled oxygen plasma. *Applied Surface Science.* **349**, 763-73 (2015).
773 [51]Kim, H. T., Jeong, O. C. PDMS surface modification using atmospheric pressure plasma.
774 *Microelectronic Engineering.* **88**, 2281-5 (2011).
775 [52]Prasad, B. R. et al. Controlling cellular activity by manipulating silicone surface roughness.
776 *Colloids and Surfaces.* **B78**, 237-42 (2010).

Figure 1

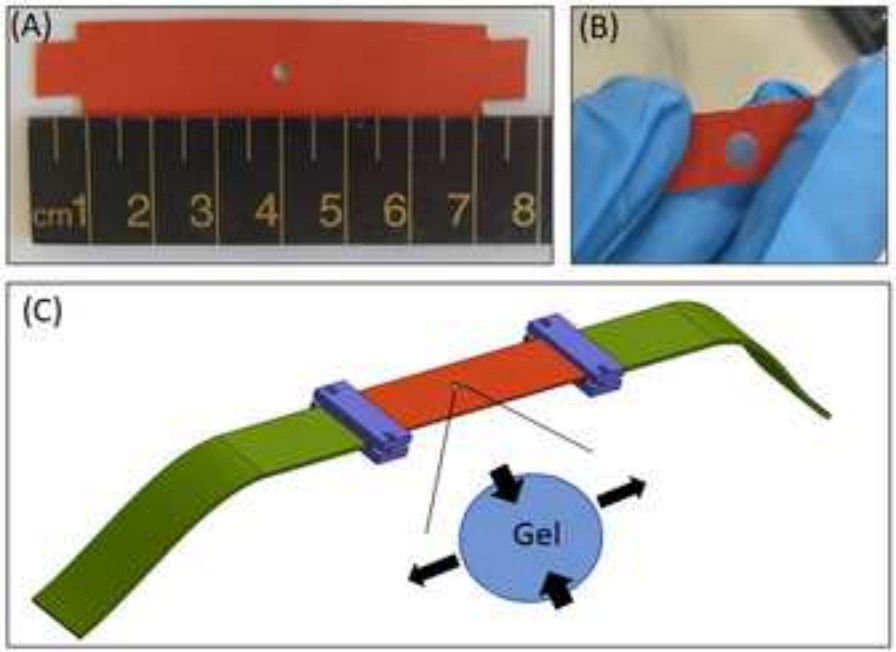

Figure 2

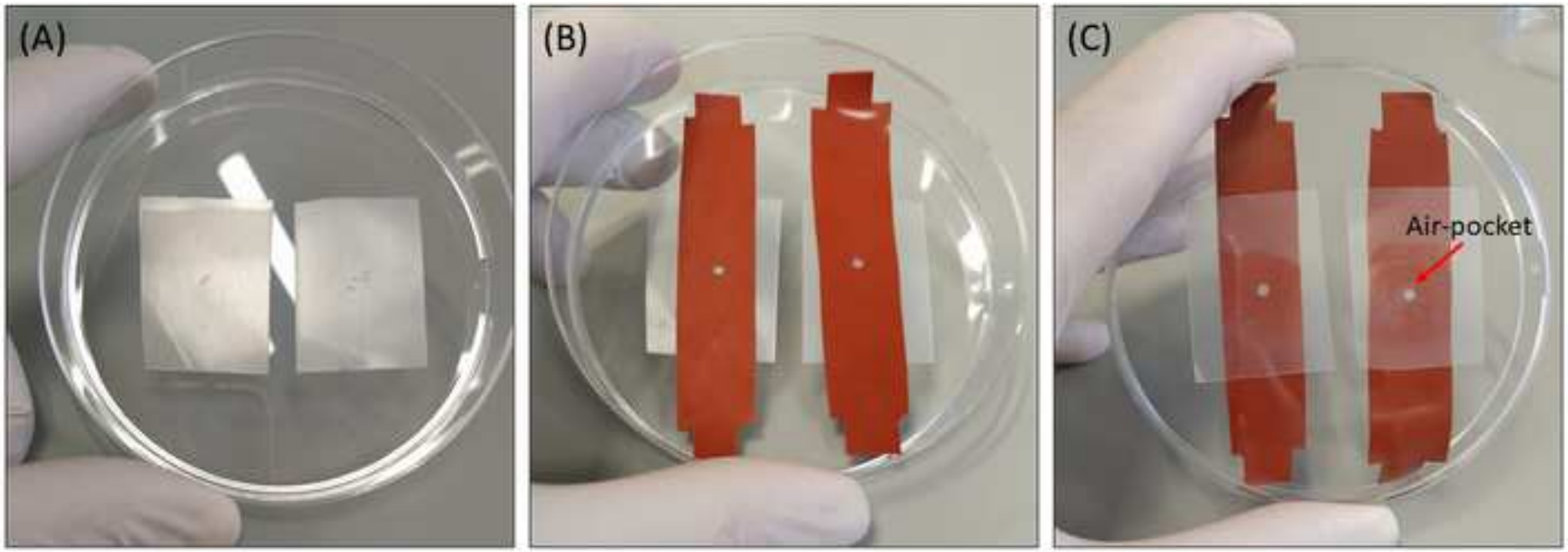

Figure 3

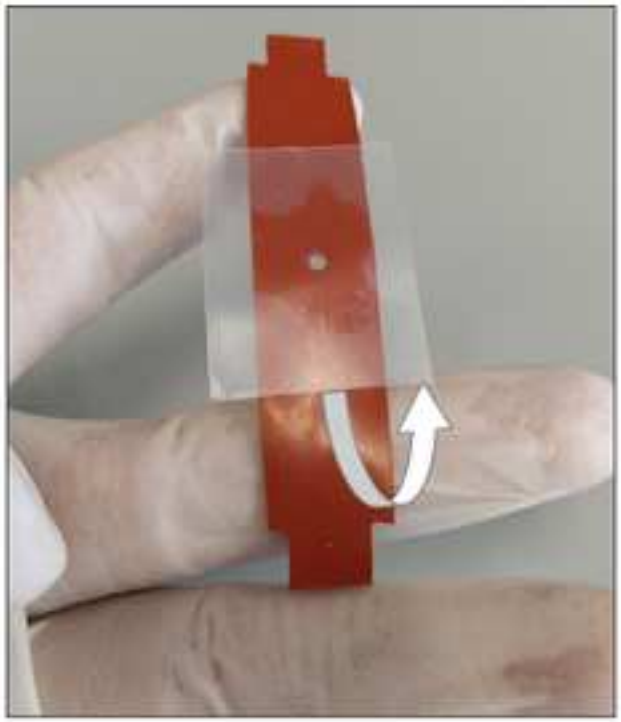

Figure 4

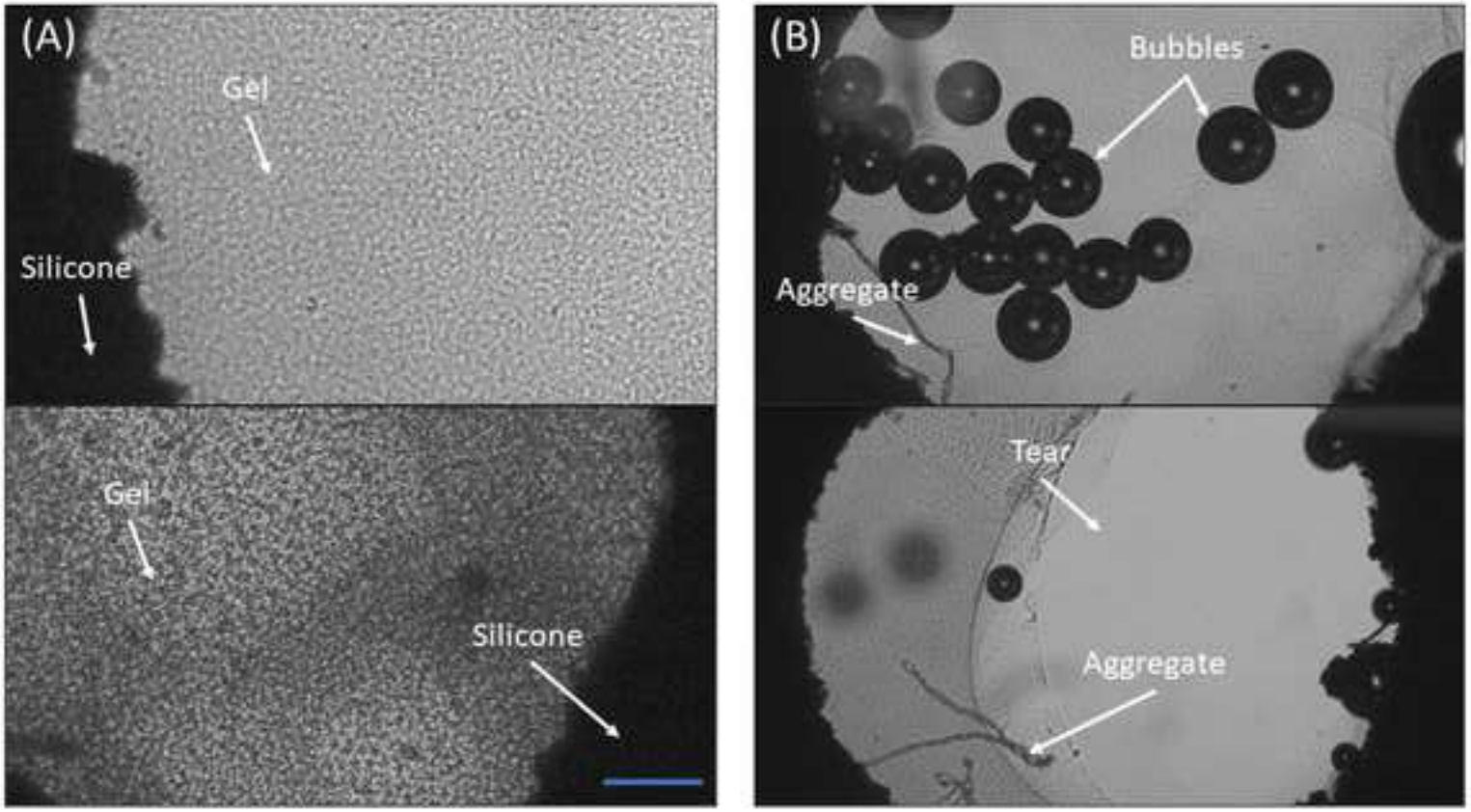

Figure 5

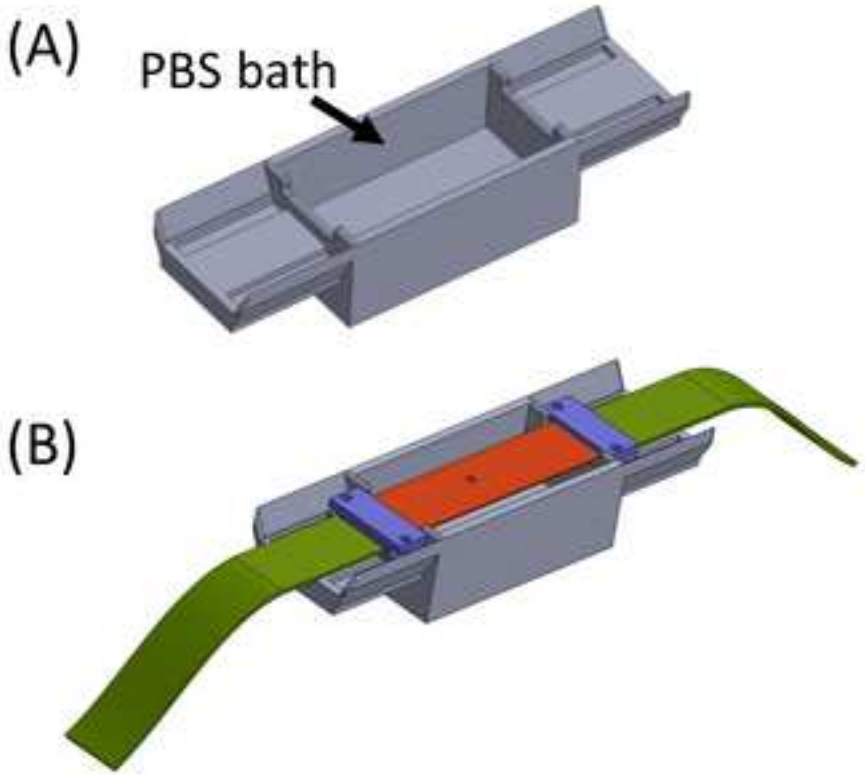

Figure 6

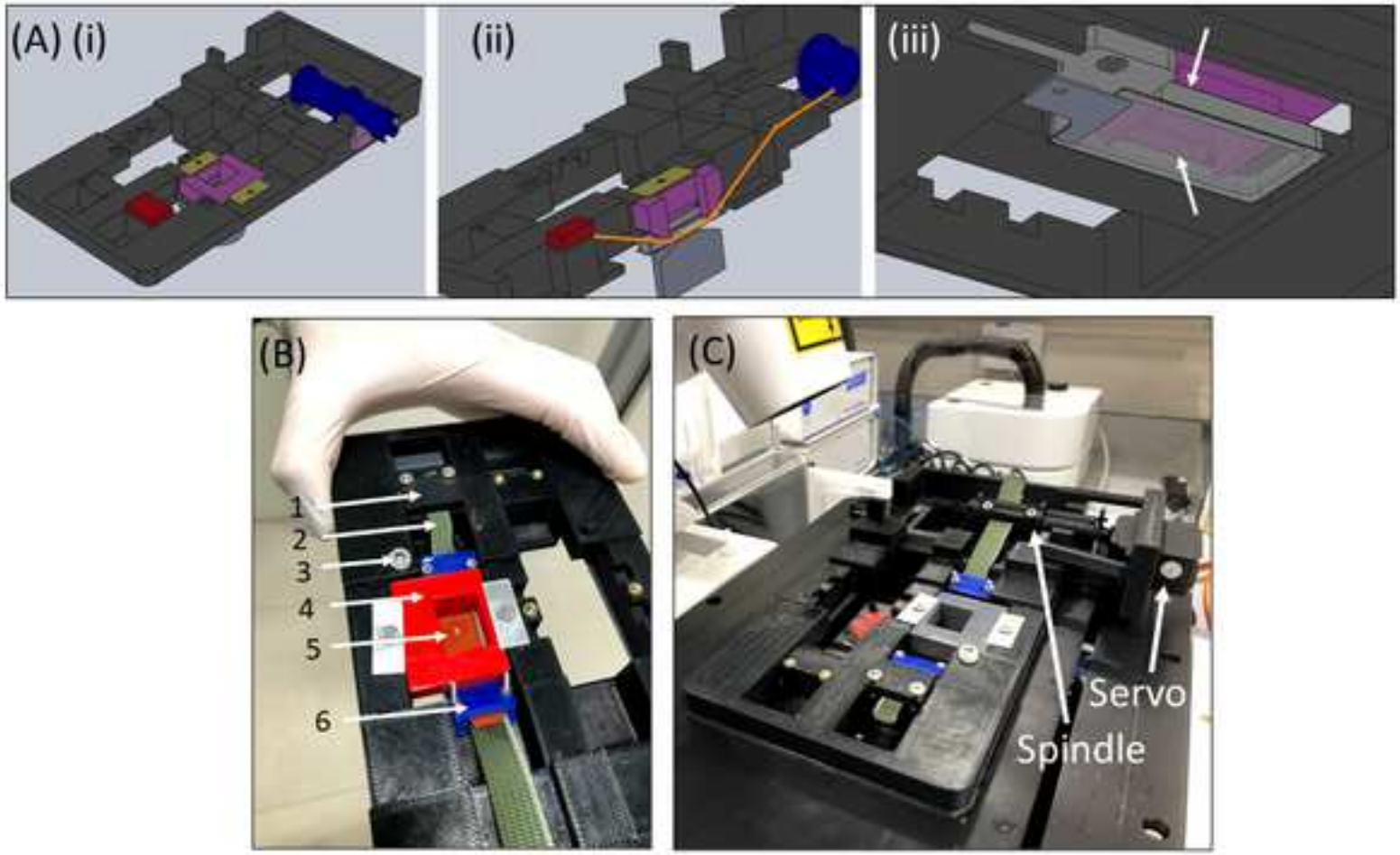

Figure 7

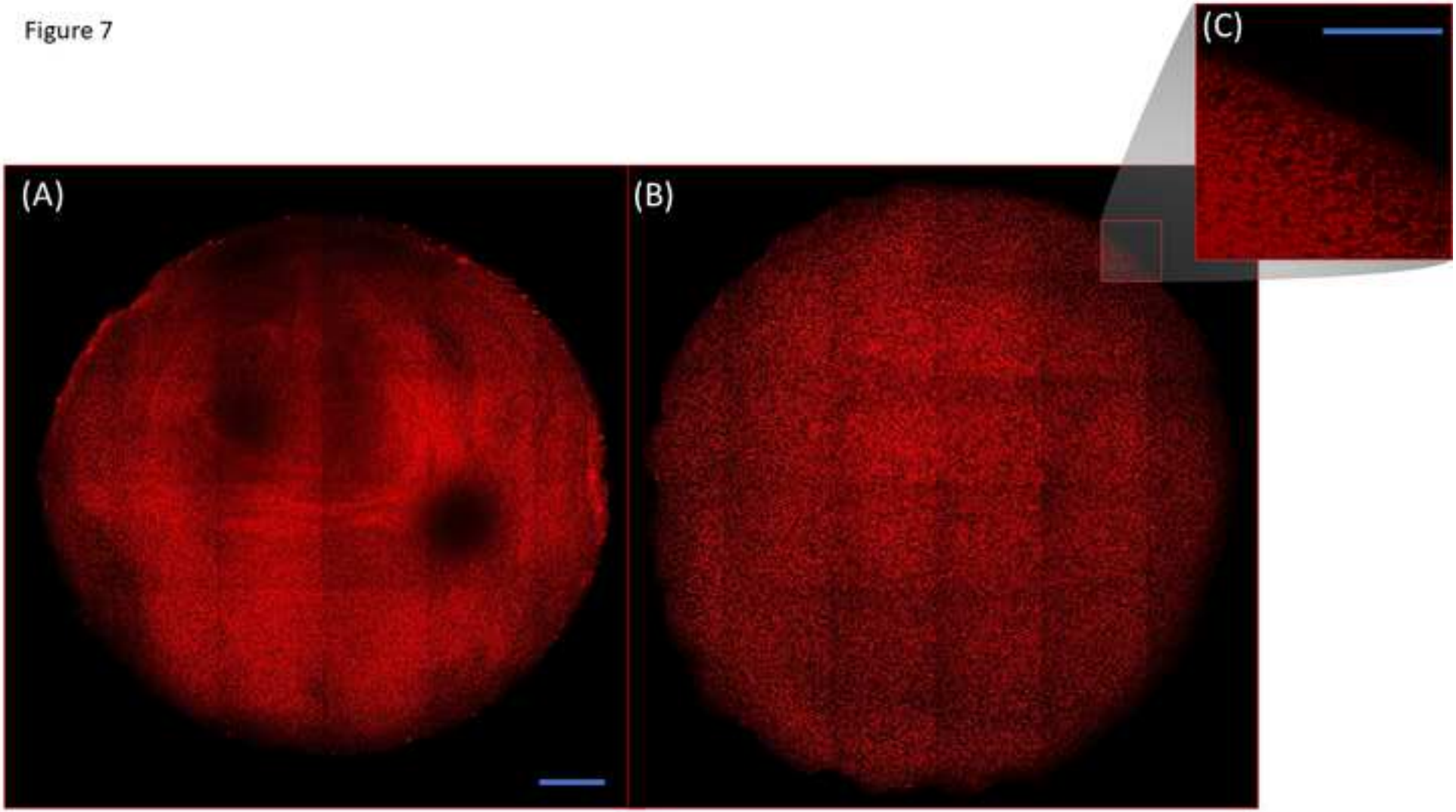

Figure 8

Figure 9

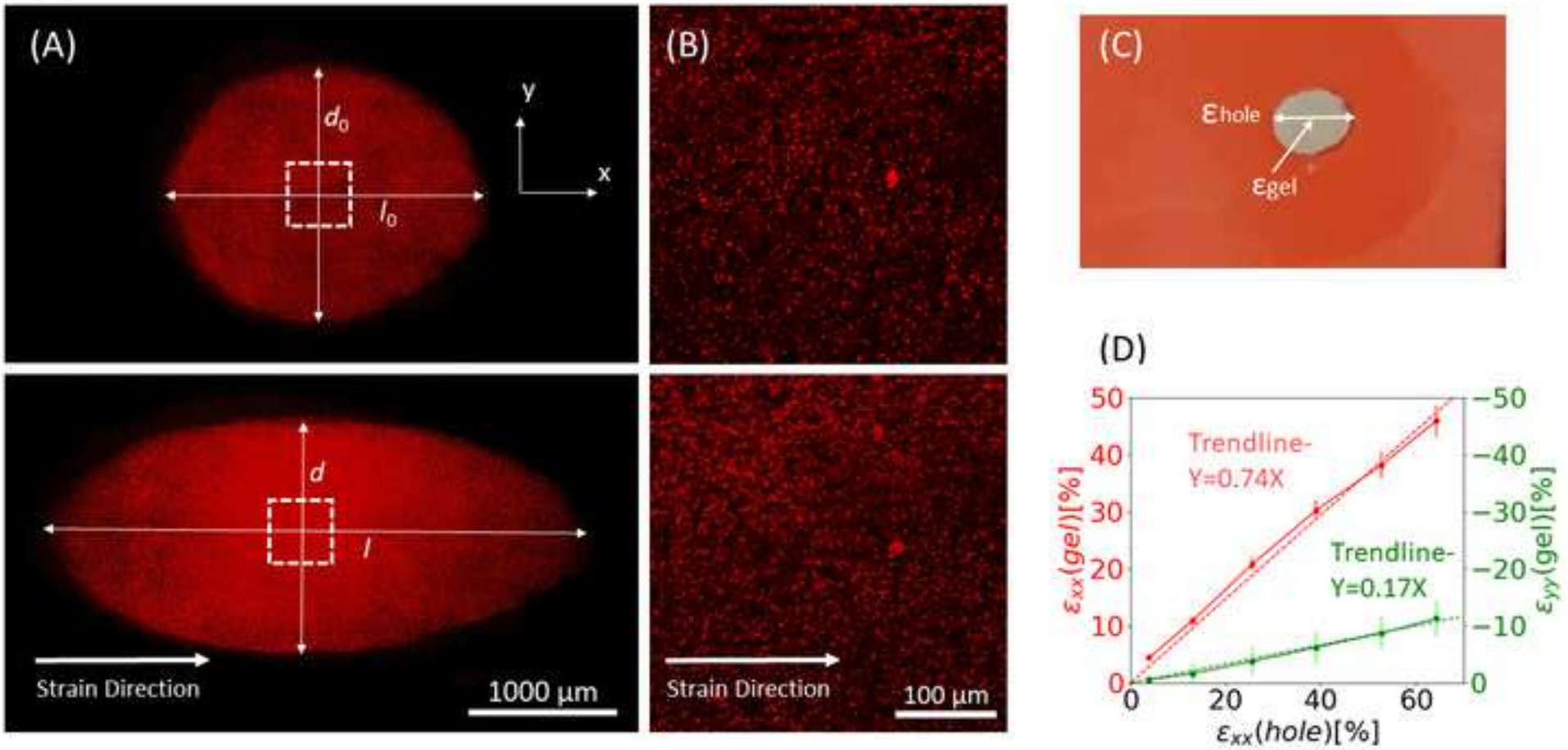

Figure 10

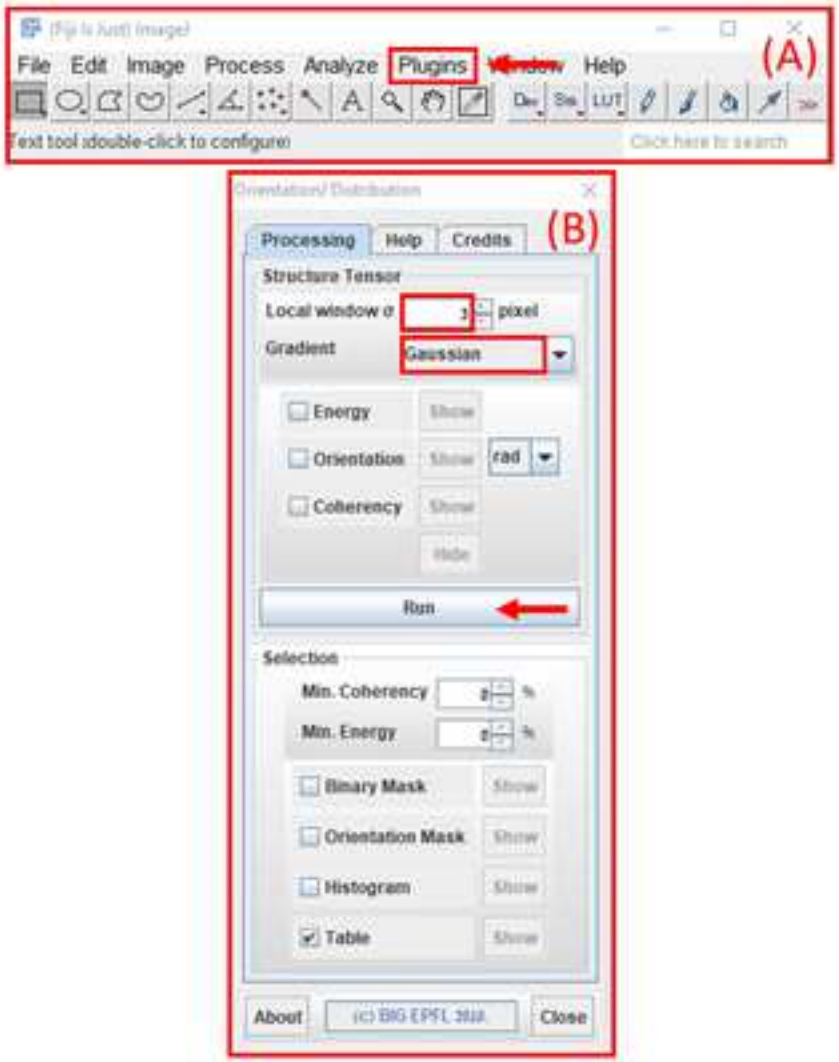

Figure 11

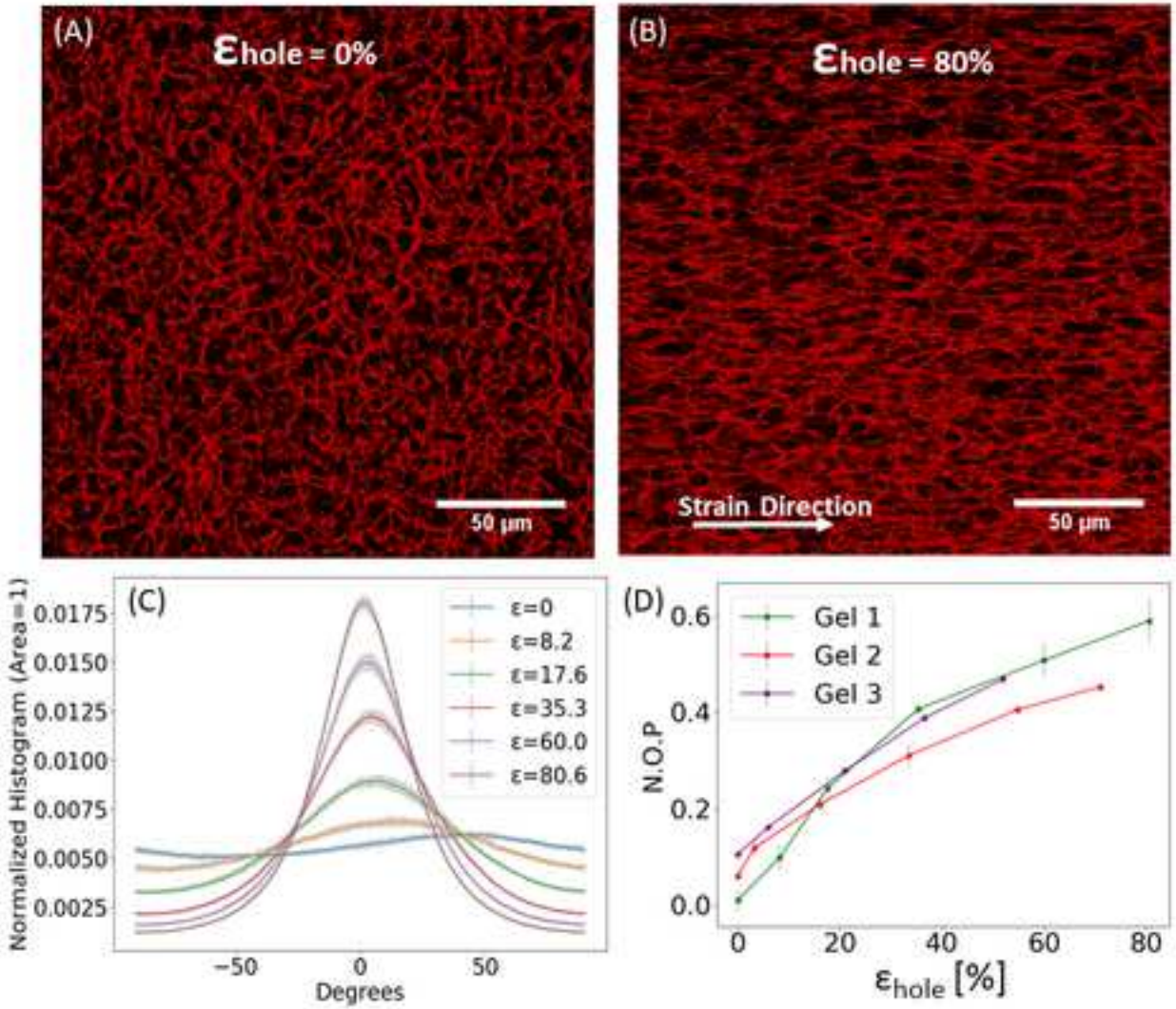

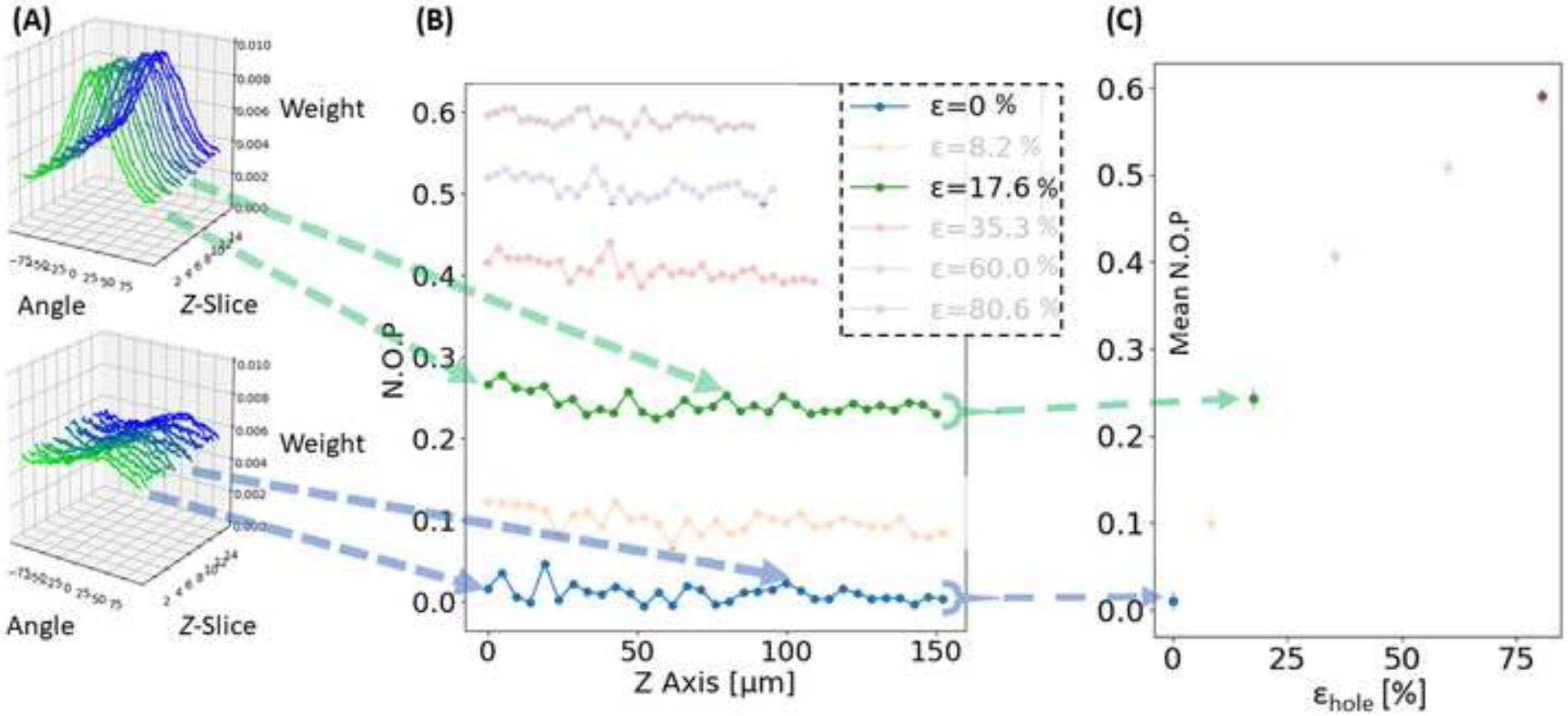

Figure 13

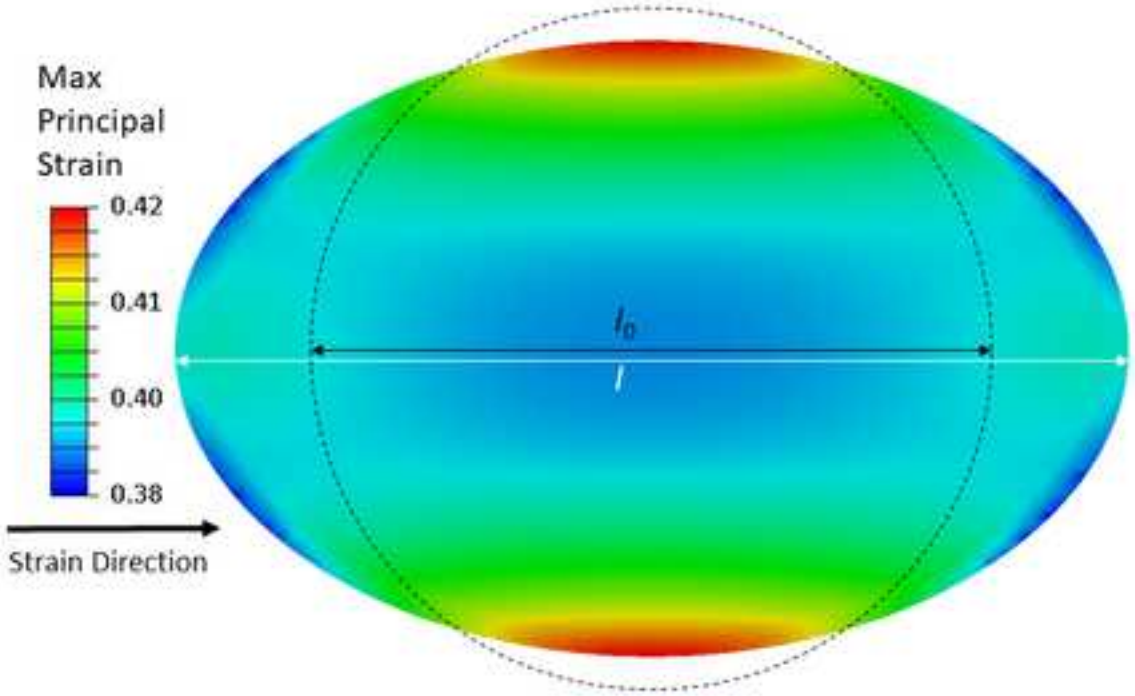

Table

Gel #1	Dynamic strain amplitude (Frequency 1 Hz)	Dynamic stretch duration (min)
	0-37%	0.1
		1
		5
		15
		30
	0-48%	1
		5
		30
	Total time under dynamic stretch	87 min

Gel #2	Dynamic strain amplitude (Frequency 1 Hz)	Dynamic stretch duration (min)
	0-30%	0
		10
		20
		30
	0-50%	30
	Total time under dynamic stretch	60 min

Gel #3	Dynamic strain amplitude (Frequency 1 Hz)	Dynamic stretch duration (min)
	0-30%	10
		20
		30
	Total time under dynamic stretch	30 min

Table of Materials

Name of Material/ Equipment	Company	Catalog Number	Comments/Description
Alexa Fluor 546 carboxylic acid, succinimidyl ester	Invitrogen	A20002	
Cell Medium (DMEM High Glucose)	Biological Industries	01-052-1A	Add 10% FBS, 1% PNS, 1% L-Glutamine, 1% Sodium Pyruvate
Cover Slip #1.5	Bar-Naor Ltd.	BN72204-30	22×40 *mm*
DIMETHYL SULPHOXIDE 99.5% GC DMSO	Sigma-Aldrich Inc.	D-5879-500 ML	
Dulbecco's Phosphate-Buffered Saline	Biological Industries	02-023-1A	
EVICEL Fibrin Sealant (Human)	Omrix Biopharmaceuticals	3902	Fibrinogen: 70 mg/mL, Thrombin: 800-1200 IU/*mL*
Fibrinogen Buffer	N/A		Recipe for 1L: 7g NaCl, 2.94g trisodium citrate dihydrate, 9g glycine, 20g arginine hydrochloride & 0.15g calcium chloride dihydrate. Bring final volume to 1L with PuW (pH 7.0-7.2)
Fluorescent micro-beads FluoSpheres (1 μm)	Invitrogen	F8820	Orange (540/560) Provided as suspension (2% solids) in water plus 2 mM sodium azide
High-Temperature Silicone Rubber	McMaster-Carr	3788T41	580 μm -thick E = 1.5 Mpa Poisson Ratio = 0.48 Tensile Strength = 4.8 MPa Upper limit of stretch = +300% engineering strain
HiTrap desalting column 5 *mL* (Sephadex G-25 packed)	GE Healthcare	17-1408-01	
HIVAC-G High Vacuum Sealing Compound	Shin-Etsu Chemical Co., Ltd.	HIVAC-G 100	
ImageJ FIJI software[39]	National Institute of Health, Bethesda, MD	Version 1.8.0_112	
Microcontroller (Adruino Uno + Adafruit Motorshield v2.3)	Arduino/Adafruit	Arduino-DK001/Adafruit-1438	
MicroVL 21R Centrifuge	Thermo Scientific	75002470	
Parafilm	Bemis	PM-996	
Primovert Light Microscope	Carl Zeiss Suzhou Co., Ltd.	491206-0011-000	
SCyUS CAD (Solidworks)	Dassault Systèmes	N/A	
SCyUS Code[37]	N/A	N/A	
Servomotor - TowerPro SG-5010	Adafruit	155	
SL 16R Centrifuge	Thermo Scientific	75004030	For 50 *mL* tubes
Sterile 10 *cm* non-culture plates	Corning	430167	
Thrombin buffer	N/A		Recipe for 1L: 20g mannitol, 8.77g NaCl, 2.72g sodium acetate trihydrate, 24 mL 25% Human Serum Albumin, 5.88g calcium chloride. Bring final volume to 1L with PuW (pH 7.0)
Trypsin EDTA Solution B (0.25%), EDTA (0.05%)	Biological Industries	03-052-1B	
USB Cable (Type B Male to Type A Male)	N/A	N/A	
Zeiss LSM 880 Confocal Microscope	Carl Zeiss AG	2811000417	
ZEN 2.3 SP1 FP3 (black)	Carl Zeiss AG	Release Version 14.0.0.0	

School of Mechanical Engineering
בית הספר להנדסה מכאנית
Iby and Aladar Fleischman Faculty of Engineering Tel Aviv University
הפקולטה להנדסה ע"ש איבי ואלדר פליישמן אוניברסיטת תל-אביב

Re: Manuscript ID JoVE61671
Journal: Journal of Visual Experiments
Title: "Controlled Strain of 3D Hydrogels under Live Microscopy Imaging"
Author(s): Avraham Kolel, Avishy Roitblat Riba, Sari Natan, Oren Tchaicheeyan, Eilom Saias, Ayelet Lesman

Vineeta Bajaj, Ph.D.
Review Editor
Journal of Visual Experiments

Date: August 28th, 2020

Dear Dr. Bajaj,

We would like to thank you for handling the submission of our manuscript and sending us the editorial and reviewer comments on our manuscript "**Controlled Strain of 3D Hydrogels under Live Microscopy Imaging**". We thank the reviewers for taking the time to provide us with their helpful suggestions, which have led to the improvement of the manuscript. Specifically, based on the reviewer's suggestions, we included 1 new figure, 1 new table, and modified several parts of the manuscript.

All changes to the manuscript are written in green. Below, we copy (in black) the reports written by the editor and reviewers, and follow them by our detailed point-by-point response (in green) to all of the issues raised by the reviewers, while quoting the modified/new text in *italic* form.

We hope that with these revisions and explanations, our updated manuscript can be accepted for publication in the *Journal of Visual Experiments*. If any further changes will be required, please do not hesitate to contact us.

We thank you in advance for your consideration.

Sincerely yours,

Avraham Kolel and co-authors

Editorial comments:

NOTE: Please read this entire email before making edits to your manuscript. Please include a line-by-line response to each of the editorial and reviewer comments in the form of a letter along with the resubmission.

• Please take this opportunity to thoroughly proofread the manuscript to ensure that there are no spelling or grammatical errors.

Response: We have proofread the manuscript.

• **Protocol Detail:** Please note that your protocol will be used to generate the script for the video, and must contain everything that you would like shown in the video. **Please ensure that all specific details (e.g. button clicks for software actions, numerical values for settings, etc) have been added to your protocol steps.** There should be enough detail in each step to supplement the actions seen in the video so that viewers can easily replicate the protocol.

Response: Details about specific button clicks were added to Protocol 7.1.1-7.1.2 for clarity. These include when to press the following buttons:

- *"Go To Zero Servo Pos"*
- *"+1"*
- *"-1"*

• **Protocol Numbering:**

1) Add a one-line space between each protocol step.

Response: We added one-line spaces between each step.

• **Protocol Highlight:** After you have made all of the recommended changes to your protocol (listed above), please re-evaluate the length of your protocol section. There is a 10-page limit for the protocol text, and a 3- page limit for filmable content. If your protocol is longer than 3 pages, please highlight ~2.5 pages or less of text (which includes headings and spaces) in yellow, to identify which steps should be visualized to tell the most cohesive story of your protocol steps.

1) The highlighting must include all relevant details that are required to perform the step. For example, if step 2.5 is highlighted for filming and the details of how to perform the step are given in steps 2.5.1 and 2.5.2, then the sub-steps where the details are provided must be included in the highlighting.

2) The highlighted steps should form a cohesive narrative, that is, there must be a logical flow from one highlighted step to the next.

3) Please highlight complete sentences (not parts of sentences). Include sub-headings and spaces when calculating the final highlighted length.

4) Notes cannot be filmed and should be excluded from highlighting.

Response: We have reviewed which sections were highlighted and added the following sections to the highlighted protocol for flow and clarity:

- Parts of Protocol 2.1
- Protocol 2.2-2.4
- The last sentence of Protocol 5.3 was highlighted
- Protocol sections 6.2-6.4 were highlighted
- Protocol 7.1, 7.1.1-7.1.2, & 7.1.4 were highlighted

• **Discussion:** JoVE articles are focused on the methods and the protocol, thus the discussion should be similarly focused. Please ensure that the discussion covers the following in detail and in paragraph form (3-6 paragraphs): 1) modifications and troubleshooting, 2) limitations of the technique, 3) significance with respect to existing methods, 4) future applications and 5) critical steps within the protocol.

Response: We ensured that this is indeed the case and made additions based on reviewer comments.

• **Figure/Table:**
1) Fig 4: Add scale bars.

Response: A scale bar was added to Figure 4, additionally, we altered the color and highlighted the relevant items for this figure in order to improve its clarity.

2) Place all legends beneath the representative results.

Response: All legends were relocated underneath the representative results.

3) Please provide each figure (if multiple panels are present per figure, keep them within 1 file) as an individual SVG, EPS, AI, TIFF, or PNG file.

Response: We will upload all figures as TIFF files.

4) Please upload only the final figure files, there seem to be some copies.

Response: We attempted to do this for our initial submission, however there were errors that were not correctable from our side. This should no longer be an issue.

• **References:**Please spell out journal names.

Response: All journal names were spelled out in full.

• **Commercial Language:** JoVE is unable to publish manuscripts containing commercial sounding language, including trademark or registered trademark symbols (TM/R) and the mention of company brand names before an instrument or reagent. Examples of commercial sounding language in your manuscript are parafilm,

Response: We have removed the following names of products:

- Parafilm
- Alexa Fluor 546
- Sephadex G-25
- Arduino

They were replaced with the following (respectively):

- Sealing film
- Fluorescent dye
- Dextran gel
- Microcontroller

• **Table of Materials:** Remove TM symbols.

Response: TM symbol was not found in the table of materials.

• If your figures and tables are original and not published previously or you have already obtained figure permissions, please ignore this comment. If you are re-using

figures from a previous publication, you must obtain explicit permission to re-use the figure from the previous publisher (this can be in the form of a letter from an editor or a link to the editorial policies that allows you to re-publish the figure). Please upload the text of the re-print permission (may be copied and pasted from an email/website) as a Word document to the Editorial Manager site in the "Supplemental files (as requested by JoVE)" section. Please also cite the figure appropriately in the figure legend, i.e. "This figure has been modified from [citation]."

Response: We have attained reprint permission and have uploaded it along with this response document and the manuscript.

Reviewers' comments:

Reviewer #1:

Manuscript Summary:

In this work Kolel et al. described in detail the method and the protocol previously used in Robia et al. (Annals of Biomedical Engineering, 2019) to perform in vitro stretching of 3D cellular constructs. The work might be of particular interest to scientists which need to investigate the role of mechanical active forces in the crosstalk between cell and the surrounding matrix. The described methodology is clear and easiest to reproduce.

Major Concerns:

None

Minor Concerns:

- In line 192 authors say that, during the preparation of hydrogel embedded with cells, cells have to be kept on ice until use: is it possible to damage cells for the low temperature or is it this passage fast? Please indicate the time.

Response: Clarified on line 183-184, "*Keep the cells chilled until use (do not exceed more than half an hour to avoid damaging the cells).*"

- Line 206/207: what is the initial solid concentration of beads used as fluorescent markers for hydrogel deformation?

Response: Solid concentration was added, "*suspension [2% solids] in water*" (line 141).

- Figure 7: apparently, it seems that there is a square grid in the gel. Is that grid the result of image stitching? If yes, please indicate the used software.

Response: Clarified on line 428-431:

- *"Tile images were captured and stitched using the confocal microscope software (See **Table of Materials**). (A) A single stitched tile Z-slice image of a fibrin gel sample with relatively homogeneous fiber density. This is an acceptable gel for stretching experiments. (B) A single stitched tile Z-slice image of a fibrin gel sample with relatively inhomogeneous fiber density due to improper thrombin and fibrinogen mixing pre-polymerization."*

In the **Table of Materials**, the software information used was added:

- *"ZEN 2.3 SP1 FP3 (black), Carl Zeiss AG, Release Version 14.0.0.0"*

- Figure 10 (Currently Figure 9): Is the accumulation of particles a consequence of compression (Poisson effect) in z-axis? Is it possible that the fluorescent signal coming from adjacent slices can affect the calculation of strain/deformation in each slice? Please, add some comments to the text. What is the optimal z-slice height for the evaluation of strain/deformation in each slice? Please, indicate these data in the manuscript.

Response: This figure is listed as 9D in the revision. Indeed, the accumulation of particles in Figure 10B is likely due to compression in the z-axis. We do not suspect that the increased bead density affects our calculation of strain, as we follow large bead aggregates and can detect them clearly after each stretch magnitude, even when the bead density is high. We comment on this issue in the revised protocol:

- A note was added to **Protocol 10** on lines 330-332: *"**NOTE**: Compression in the Z-direction (Poisson effect) can lead to an increase in bead density as stretch increases, therefore we suggest choosing bead aggregates large enough so they are clearly identifiable."*

We have chosen the Z-slice height for strain evaluation in the center of gel. This allowed us to return to the same z-slice after each stretch magnitude. We comment on it in the revised protocol

- A note was added to **Protocol 6** on lines 259-262: *"**NOTE**: At different XY locations, the thickness of the gel can vary. This section of the protocol measures the minimum thickness of the gel, allowing us to determine the gel quality and indicate if it is sufficient for stretching. Additionally, finding the center of the gel provides a reference point to return to post-stretching, whether static or dynamic."*

- The graph in Fig. 10D (Currently Figure 9D) indicates that the hole deformation exx(hole) is almost completely transferred to the gel exx(gel), nevertheless the measurements of exx(gel) have been performed by considering only few pairs of particles/aggregates of particles. It is not clear if inside the gel gradients of strain can arise or if strain is homogeneously distributed Quantifying the deformation field by performing a traction force microscopy experiment would clarify this point.

Response: This figure is now listed as 9D in the revision. Indeed, measuring the internal strain gradients in the gel is an important level of resolution to our system. However, it has remained challenging for us to measure it due to the movement of the gel in the x (displacement) and z (compression) axes under microscopy during stretch. For this reason, we performed finite element simulations in order to provide prediction for the internal strains. We added **Figure 13** to provide a portion of these results and discussed it in the results and discussion sections. The additions are listed below:

- In the results section, lines 374-380: *"Since it has proven difficult to perform in-depth analysis of the internal strains in the entire gel, we provide here preliminary results of finite element (FE) simulations performed on 2D continuous material given the mechanical properties of fibrin (**Figure 13**). The external strain of the cut-out is ~40% and the color-map represents the stretch-induced strain field. The color-map ranges from 38%-42%, indicating that gel strains are relatively homogenous throughout the circular gel area. We note that if other gel*

geometries are used, gradients in strain may arise, and this is a topic for future studies."

- And in the discussion section, lines 522-526: *"In the current protocol, we focused only on gels in a circular geometry. Under such conditions, internal strains are relatively homogeneous throughout the gel, as predicted by our FE simulations (**Figure 13**). However, if other gel geometries will be considered by modifying the cut-out section of the silicone, gradients will emerge."*

Typos:
- Line 87: 1 KPa → 1 kPa.
- Line 128: 2.5 um → 2.5 ul.
- Line 129: 1 um → 1 ul.
- Line 144: soak in NaOH 0.2 M, for 0.5 hour… → soak in 0.2 M NaOH for 0.5 hour, …

Response: Typos were fixed.

Reviewer #2:
Manuscript Summary:
In this article, the authors present an elastic silicone strips based method that allows external stretching of 3D soft hydrogels. The stretching system can be easy to replicate in other labs with common laboratory instruments. The combination of confocal microscopy gives the system the ability to observe and analyze the hydrogel fiber structure and cell morphology in real time, which may have great application potential in investigation of 3D cell culturing under dynamic stretch. There are several comments from this reviewer that need to be addressed before this paper could be considered further.

Major Concerns:

Lack of experiments results on cell cultured in this system.

Although author has declared that the gel can keep adhesion over a period of 5 hours under a static stretch of 10%, it is still quite short compare the common cell culture period (3 to 7 days).

Response: The reviewer is correct that 5 hours is relatively a short period for cell culture. We are currently testing longer adhesion times for cell culturing in order to improve our methodology. In ongoing experiments in our lab, we have demonstrated the adhesion of cell-laden fibrin gel to the silicone strip for over two days. These data will be published in future work.

The author didn't demonstrate the adhesion of gel under dynamic stretch and the gels is very likely to fall off in this situation. If the system can only be used for static stretch, there have been many alternative existing methods available for researchers.

Response: We thank the reviewer for highlighting this issue. To respond to this comment, we performed dynamic stretch tests and provided the results in **Table 1**. Additionally, we added the following paragraph to the representative results section on lines 381-386:

- *"In order to demonstrate that embedded fibrin gels can sustain adhesion to the silicone strip at high strains (0 to +30%) and frequencies (up to 1 Hz), we ran preliminary tests (protocol for this test is not included in this work) showing no detachment of the gels from the inner walls of the cut-out. Three gels were tested, gel 1 for a total duration of ~87 minutes, gel 2 for 60 minutes & gel 3 for 30 min total (**Table 1**). In all three of these cases fibrin hydrogels maintained their adhesion."*

- A legend was also added for **Table 1** on lines 477-480: *"**Table 1**: Representative results of dynamic stretch proof of concept. Three gels were embedded in silicone strips and stretched dynamically (1 Hz) for various durations. Strains ranged from zero to various magnitudes above 30%. All three gels of these successfully sustained their adhesion to the inner walls of the circular cut-out of the silicone strip."*

We also made some changes and additions to the discussion on lines 514-520:

- *"(i) Application of a cyclic stretch regime to cell embedded hydrogels. As dynamic movement of the motor is encoded by the microcontroller software, any cyclic profile can be programmed, constrained only by the resolution and the rotation speed of the motor employed in the system (more details available in Roitblat Riba et al.[41]). In this work, we demonstrated that fibrin gel can sustain adhesion under dynamic stretch (**Table 1**). Though further testing is necessary, the application of cyclic loading would give insights into the dynamic response of the hydrogel and embedded cells to external cyclic loading."*

Minor Concerns:
Gels under stretch undergo inhomogeneous force application and strain. The image analyses of strain field are great in this article while the force analysis is insufficient.

Response: In order to measure the force (or stress) from the strain field, we need to know the elastic moduli at each point. This information is currently not available to us; therefore, we were not able to assess the local forces acting in the gel.

The punched hole in the center of the silicone strips is 2 mm and the thickness of the silicone strips is 0.5mm. Under such scale of hydrogel thickness, the exchange of nutrition and metabolite in 3D cultured system may not be easily.

Response: The reviewer is correct that restricted diffusion of nutrients poses a big challenge in engineering thick tissues. Typically, this is addressed in the tissue engineering field by incorporating blood vessels in the 3D constructs. However, dealing with this issue is not the focus of the current protocol.

Reviewer #3:
Manuscript Summary:
The authors present a stretching technique to deform gels or tissues. It allows stretching very soft gels (100Pa) and couple confocal microscopy which requires very thin systems. The gels are homogeneously deformed and acquired images show a good reliability of the method. In particular sof fibrin gels contain fibers that are aligned nicely.
It is not quite novel, as previous authors already suggested such methods (Vader et al, PLOS One 2009, reference 5). But this is not a requirement for this type of journal. The authors could have shown what happens when including cells within the gel, as

this is a very important perspective.
As a consequence I do recommend publication.

Response: We thank the reviewer for their recommendation. In Roitblat et al. 2019 we discuss the ability of culturing of cells embedded in fibrin gels while using this stretching protocol. The response of cells to external stretch will be analyzed in future studies.

Vader et al. shows a method to pull from two single points inducing local stretch in the gel. Our method allows for stretch from the entire circumference of the gel, generating deformation throughout the entire gel. We made this point clearer in the Introduction on lines 69-71: *"Some techniques generate stretch that locally deforms the 3D gel, for example by pulling needles from two single points in the gel,[5] while other techniques deform the entire bulk of the gel[16]."*

[5] Vader, D., Kabla, A., Weitz, D., Mahadevan, L. Strain- induced alignment in collagen gels. PLoS ONE. 4, 5902. (2009).

[16] Wang, L., Li, Y. H., Chen, B., Liu, S. B., Li, M. X., Zheng, L., Wang, P. F., Lu, T. J., Xu, F. Patterning cellular alignment through stretching hydrogels with programmable strain gradients. ACS Applied Materials & Interfaces. 7, 15088–15097. (2015).

Minor Concerns:
Lots of figures appear twice. e.g. Fig1 and Fig5 etc.

Response: This was due to uploading errors, which are corrected in the revision submission.

Reviewer #4:
Manuscript Summary:
In this manuscript, Kolel et. al describe the protocol based largely on their previous study (Roitblat, 2019) on how to stretch fibrin gels using elastic silicon strips. Their approach uses low volume gels (~3.5 uL) and can measure soft gels (0.1 kPa). Some suggestions to improve the manuscript.

Minor Concerns:
1. In the introduction it would be worthwhile a paragraph explaining the mechanism behind the reaction between fibrogen and thrombin to form fibrin gels.

Response: The introduction focuses on the ECM and hydrogels in general and not specifically on fibrin since our method could in principle be used for other types of hydrogels, such as collagen. Therefore, we preferred not to mention this specific information about fibrin.

2. An important factor in this method is the elasticity of the silicon band. What is its Young's modulus? How does this impose the upper measurable limit for this approach?

Response: The mechanical properties of the silicone rubber were added to the **Table of Materials.** The mechanical properties of the silicone rubber do not limit our ability to stretch the gel, as the silicone is much more elastic than the gel. They are listed in the table of materials as followed:

-E = 1.5 MPa

-Poisson Ratio of 0.48
-Upper limit of stretch = +300% engineering strain
-Tensile Strength = 4.8 MPa

3. I could not find a step or note on how the authors verify that the gel edges do not detach under strain.

Response: Under fluorescent microscopy, detachment can be detected visually because the fibers are fluorescently labeled, and the silicone appears as dark. A step for ensuring no detachment under strain was added (**Protocol 7.2**):

- On lines 289-293: *"7.2. At each stretch magnitude where analysis is desired, capture a single Z-slice high-resolution tile image of the entire gel area for post-processing analysis. Similar to **Protocol 6.2**, verify that the gel has not detached from the silicone throughout its circumference by scanning the interface between the gel (red) and the silicone (dark background), looking for changes in the adhesion from the previous stretch magnitude."*

- Additionally, we added a similar step for pre-strain in Protocol 6.2 on lines 247-249: *"To determine full adhesion of the gel to the silicone throughout its circumference, scan the interface of the fluorescent label of the gel and the silicone strip (dark background) under the microscope (**Figure 7C**)."*

A zoom in microscope image of the interface between the gel and the silicone was also added to **Figure 7** (**Figure 7C**) and the following text was added to the legend of figure 7 on lines 433-435:

- *"(C) Zoom in of the interface between the fluorescently labeled gel (red) and the silicone (black background). Scale bar = 100 μm."*

4. I think it would be a good idea to already mention the fluorescent beads in step 1.3 Now it appears first time as a note after step 4.2. Also it is not clear if beads are present when measuring cells or if the beads are always present?

Response: The step is clarified to mention that beads are an entirely separate experiment from the cells. The note was moved to follow step **Protocol 1.3** and a clarification was added to the note on line 143-144: "*Beads should be included only when internal strain measurements are desired, either in the presence or absence of cells.*"

5. Put scale bar in Figure 4.

Response: A scale bar was added.

6. Fig 5 (page 29) does not correspond to the caption.

Response: A problem occurred with uploading the submitted figures. This was corrected in the revision submission.

7. The height of gel seems to be measured in a single XY point. How does it vary when scanning around the gel? Height is particularly important for determining visco-elastic properties.Step 7.1.3. - what is the step size during Z-slicing?

Response: The height of the gel is not completely uniform throughout the gel. However, the main goal of this step was to measure the minimum thickness of the gel, which allows us to determine the gel quality and indicate if it is sufficient for

stretching. A note was added on line 259-262 clarifying this point, "***NOTE**: At different XY locations, the thickness of the gel can vary. This section of the protocol measures the minimum thickness of the gel, allowing us to determine the gel quality and indicate if it is sufficient for stretching.*"

Additionally, we added a step size recommendation for z-slicing on lines 241-242, *"(≤10 Z-slices with a step size of approximately 10 μm is sufficient)"*

8. Since the Z-measurement takes 20-30 min, especially at high strains, how does the viscoelasticity influence the reproducibility of the measurements? If the authors repeat the measurement in the same spot, how does N.O.P. vary? Were the error bars in Fig 12 obtained from the same spot, same gel?

Response: In our experience, the characteristic time for the gel to stabilize is only a few seconds and the data collection is on the order of tens of minutes, so viscosity behavior has negligible effects if any at all. We have repeated image capture at various time points of the same location (XY) in the same gel after stretch with little to no variation in fiber alignment.

In reference to the error bars, they reflect the variation in the fiber alignment between all the z-slices in an individual stretch magnitude. The same XY point (center of the gel) is selected each time. We now define the error bars in the figure legend on line 470-471, *"Error bars represent the standard deviation of NOP for all the Z-slices in an individual stretch magnitude at the same XY point in the same gel."*

9. Define theta in eq. (4).

Response: We obtained a distribution of angles as an output from the OrientationJ plug-in for ImageJ, this is measured using pixel gradients in the image. We added a definition in lines 322-324, "*The orientation angle, θ, is the fiber angle in relation to the strain axis (x-axis) obtained through image analysis and precisely defined in the OrientationJ documentation.*[40]"

[40] EPFL Switzerland. OrientationJ plug in. (2019).

10. Fig 12C is cut out.

Response: This problem was fixed.

11. The authors claim that their method can strain gels in 3D. While the gels are attached in the cylinder inside the silicone matrix, I think the strain is only in 2D - so page 13 last paragraph seems incorrect.

Response: The reviewer is correct that the strain is applied in 2D, but it acts on a 3D hydrogel. Therefore, we corrected it to better represent what our system is accomplishing (alteration found on line 488).

Originally we wrote, "*The major advantages of the presented method over existing approaches include the possibility to strain very soft hydrogels (Elastic Modulus of ~100 Pa) in three-dimensions (from the circumference of the gel), and under live confocal imaging".*

It was replaced by, *"The major advantages of the presented method over existing approaches include the possibility to strain very soft 3D hydrogels from their circumference (Elastic Modulus of ~100 Pa), and under live confocal imaging."*

12. Table of materials: I could not find on McMaster-Carr a product with Cat. No. RC00113P. Check if this is correct for the silicone rubber.

Response: We thank the reviewer for catching this oversight. The catalog number was corrected to reflect McMaster-Carr's online catalog (Cat. No. 3788T41).

Also add cat. Nos. for Fibrinogen and Thrombin.

Response: This information is available under the "EVICEL" entry in the table of materials. Both fibrinogen and thrombin are purchased together in the EVICEL packaging.

Reviewer #5:

Manuscript Summary:
The authors describe a detailed protocol to perform stretching of biological hydrogels like fibrin, while assessing strain in the XY and Z directions. It is well written and detailed. A few minor corrections needed.

Major Concerns:
CAD files needed to reproduce the 3D prints should be included given this is a methods journal.

Response: We did attach these files with our submission, and they will be included in the supplementary materials of the publication. We also mention this in the original manuscript at the beginning of the discussion section. In the revision this can be found in lines 484-485:

"We include here the full computer-aided design (CAD), Python and microcontroller codes of the SCyUS device."

Minor Concerns:
Delete "novel" from abstract and manuscript

Response: The word "novel" was removed.

There are commercially available devices for stretching 3D gels and/or engineered tissues. Can the authors acknowledge these devices in their manuscript? I'm confident the authors' approach is cheaper, and more adaptable, but the availability of commercial products is important to acknowledge.

Response: Commercially available devices are acknowledged in the introduction, lines 66-67, *"Methods and devices that allow for 3D sample stretching include both commercially available[24,25,26,27,28] and those developed for laboratory research.[29]"*

- We added references to these commercially available devices:

[24] Flexcell. Linear Tissue Train® Culture Plate. 2019.

[25] Flexcell. Tissue Train®. 2019.

[26] CellScale. MCT6 Stretcher. (Originally was reference #27)

[27] STREX. STB-150. 2019.

[28] STREX. Stretch Chambers. 2019.

Pg 3 line 123-125: it would be helpful if the authors mentioned how large their typical fibrin gel is, so that the reader can infer what percent of overall polymer should be labeled.

Response: On line 196 we indicate the final volume of a typical fibrin gel (5 μL) made using this protocol. We also note that the labeling occurs only on the fibrinogen and provide the protocol for this on lines 107-133 (**Protocol 1.1-1.2**). The labeled fibrinogen exactly half of the final polymer (2.5 μL)

Pg. 3 line 128-129: the authors have written um ("microns") but I think this should say "mL" or "micro-liters"?

Response: The typo was fixed. Thank you for this correction.

Lines 139-145: Can biopsy punches be used?

Response: Absolutely, this is a great idea, we thank the reviewer for this input. We have not yet attempted using a biopsy punch, but it is something we will try in future work.

Can the silicone strips be autoclaved?

Response: We generally sterilize the strips using UV and ethanol; however, it can be autoclaved since the material is capable of withstanding between -73 °C – +260 °C. A typical autoclave sterilization cycle reaches only 140°C. A note was added on line 179-180 to reflect this:

*"**NOTE**: Alternatively, an autoclave sterilization cycle (140 °C) can be performed on the silicone strips since they are resistant to up to 260°C."*

What size fluorescent beads do the authors use, and what's the source?

Response: The beads are 1 micron in diameter Carboxylate-modified spherical particles and are made from polystyrene.

The specific product can be found in the **Table of Material** and more information is available on the producer's website at:
https://www.thermofisher.com/order/catalog/product/F8820#/F8820

We mention the bead size in line 141:

*"**NOTE**: In order to perform internal strain analysis, 1 µm diameter fluorescent spherical beads (purchased as a suspension [2% solids] in water plus 2 mM NaN3)…"*

And again on line 351:

*"Representative data from static stretch of increasing magnitudes applied to the silicone strip carrying a 3D fibrin hydrogel, embedded with 1 µm fluorescent beads, is shown in **Figure 9**."*

Reviewer #6:
Manuscript Summary:
The authors present a clear and well written protocol for the application of controlled strain to 3D hydrogels under live imaging. They demonstrate the ability to track fluorescently labelled beads on the length scale of a cell, and track the alignment of fluorescently labelled fibres in the strained hydrogel. This is all based on the prior

work of the authors presented in ref 37. This manuscript with accompanying video when that is produced will likely be of benefit to those working on the role of mechanobiology in regulating cell-ECM interactions and ECM remodelling.

Major Concerns:
None

Minor Concerns:
1. Introduction, line 47: Reference 3 does not refer to tissue remodelling, but cell remodelling. Please use a more appropriate reference.

Response: The citation was replaced with *"[3] Grodzinsky et al. 2000, Cartilage Tissue Remodeling in Response to Mechanical Forces"*, which specifically refers to tissue remodeling.

2. Introduction, line 59: Reference 5 does not use PDMS to examine cell reorientation.

Response: We thank the reviewer for noticing this oversight, Reference 5 was removed from this line.

3. Figure numbers in the reviewer pdf are out of sync.

Response: This was due to an upload error and the problem has been fixed.

4. The edge of Figure 12C is missing.

Response: The figure was corrected.

SPRINGER NATURE LICENSE TERMS AND CONDITIONS

Aug 02, 2020

This Agreement between Tel Aviv University -- Avraham Kolel ("You") and Springer Nature ("Springer Nature") consists of your license details and the terms and conditions provided by Springer Nature and Copyright Clearance Center.

The publisher has provided special terms related to this request that can be found at the end of the Publisher's Terms and Conditions.

License Number	4831521106459
License date	May 17, 2020
Licensed Content Publisher	Springer Nature
Licensed Content Publication	Annals of Biomedical Engineering
Licensed Content Title	Straining 3D Hydrogels with Uniform Z-Axis Strains While Enabling Live Microscopy Imaging
Licensed Content Author	Avishy Roitblat Riba et al
Licensed Content Date	Dec 4, 2019
Type of Use	Journal/Magazine
Requestor type	academic/university or research institute
Is this reuse sponsored by or associated with a pharmaceutical or a medical products company?	no
Format	electronic
Portion	figures/tables/illustrations
Number of figures/tables/illustrations	5
Will you be translating?	no
Circulation/distribution	50000 or greater
Author of this Springer Nature content	yes
Title of new article	Controlled Strain of 3D Hydrogels under Live Microscopy Imaging
Lead author	Avraham Kolel
Title of targeted journal	Journal of Visual Experiments
Publisher	MyJove Corp
Expected publication date	Aug 2020
Portions	We would like to reuse or modify Figures 2, 3, 5, 6, and S3. In Addition we would like to add downloadable CAD and Code files in the online

	publication to allow for the reproduction of our method.
Additional Information	This is a visual online journal where we are presenting the method we used in Roitblat Riba et al.
Requestor Location	Tel Aviv University Wolfson Mechanical Engineering Building Room 331 Ramat Aviv , 6997801 Israel Attn: Tel Aviv University
Billing Type	Invoice
Billing Address	Tel Aviv University Kehilat Kovna 4 Apt. 6 Tel Aviv, Israel 6940063 Attn: Tel Aviv University
Total	0.00 USD

Terms and Conditions

Springer Nature Customer Service Centre GmbH
Terms and Conditions

This agreement sets out the terms and conditions of the licence (the **Licence**) between you and **Springer Nature Customer Service Centre GmbH** (the **Licensor**). By clicking 'accept' and completing the transaction for the material (**Licensed Material**), you also confirm your acceptance of these terms and conditions.

1. **Grant of License**

    1. The Licensor grants you a personal, non-exclusive, non-transferable, world-wide licence to reproduce the Licensed Material for the purpose specified in your order only. Licences are granted for the specific use requested in the order and for no other use, subject to the conditions below.

    2. The Licensor warrants that it has, to the best of its knowledge, the rights to license reuse of the Licensed Material. However, you should ensure that the material you are requesting is original to the Licensor and does not carry the copyright of another entity (as credited in the published version).

3. If the credit line on any part of the material you have requested indicates that it was reprinted or adapted with permission from another source, then you should also seek permission from that source to reuse the material.

2. **Scope of Licence**

1. You may only use the Licensed Content in the manner and to the extent permitted by these Ts&Cs and any applicable laws.

2. A separate licence may be required for any additional use of the Licensed Material, e.g. where a licence has been purchased for print only use, separate permission must be obtained for electronic re-use. Similarly, a licence is only valid in the language selected and does not apply for editions in other languages unless additional translation rights have been granted separately in the licence. Any content owned by third parties are expressly excluded from the licence.

3. Similarly, rights for additional components such as custom editions and derivatives require additional permission and may be subject to an additional fee. Please apply to Journalpermissions@springernature.com/bookpermissions@springernature.com for these rights.

4. Where permission has been granted **free of charge** for material in print, permission may also be granted for any electronic version of that work, provided that the material is incidental to your work as a whole and that the electronic version is essentially equivalent to, or substitutes for, the print version.

5. An alternative scope of licence may apply to signatories of the STM Permissions Guidelines, as amended from time to time.

- **Duration of Licence**

1. A licence for is valid from the date of purchase ('Licence Date') at the end of the relevant period in the below table:

Scope of Licence	Duration of Licence
Post on a website	12 months
Presentations	12 months
Books and journals	Lifetime of the edition in the language purchased

- **Acknowledgement**

1. The Licensor's permission must be acknowledged next to the Licenced Material in print. In electronic form, this acknowledgement must be visible at the same time as the figures/tables/illustrations or abstract, and must be hyperlinked to the journal/book's homepage. Our required acknowledgement format is in the Appendix below.

- **Restrictions on use**

1. Use of the Licensed Material may be permitted for incidental promotional use and minor editing privileges e.g. minor adaptations of single figures, changes of format, colour and/or style where the adaptation is credited as set out in Appendix 1 below. Any other changes including but not limited to, cropping, adapting, omitting material that affect the meaning, intention or moral rights of the author are strictly prohibited.

2. You must not use any Licensed Material as part of any design or trademark.

3. Licensed Material may be used in Open Access Publications (OAP) before publication by Springer Nature, but any Licensed Material must be removed from OAP sites prior to final publication.

- **Ownership of Rights**

1. Licensed Material remains the property of either Licensor or the relevant third party and any rights not explicitly granted herein are expressly reserved.

- **Warranty**

IN NO EVENT SHALL LICENSOR BE LIABLE TO YOU OR ANY OTHER PARTY OR ANY OTHER PERSON OR FOR ANY SPECIAL, CONSEQUENTIAL, INCIDENTAL OR INDIRECT DAMAGES, HOWEVER CAUSED, ARISING OUT OF OR IN CONNECTION WITH THE DOWNLOADING, VIEWING OR USE OF THE MATERIALS REGARDLESS OF THE FORM OF ACTION, WHETHER FOR BREACH OF CONTRACT, BREACH OF WARRANTY, TORT, NEGLIGENCE, INFRINGEMENT OR OTHERWISE (INCLUDING, WITHOUT LIMITATION, DAMAGES BASED ON LOSS OF PROFITS, DATA, FILES, USE, BUSINESS OPPORTUNITY OR CLAIMS OF THIRD PARTIES), AND
WHETHER OR NOT THE PARTY HAS BEEN ADVISED OF THE POSSIBILITY OF SUCH DAMAGES. THIS LIMITATION SHALL APPLY NOTWITHSTANDING ANY FAILURE OF ESSENTIAL PURPOSE OF ANY LIMITED REMEDY PROVIDED HEREIN.

- **Limitations**

1. ***BOOKS ONLY:***Where '**reuse in a dissertation/thesis**' has been selected the following terms apply: Print rights of the final author's accepted manuscript (for clarity, NOT the published version) for up to 100 copies, electronic rights for use only on a personal website or institutional repository as defined by the Sherpa guideline (www.sherpa.ac.uk/romeo/).

- **Termination and Cancellation**

1. Licences will expire after the period shown in Clause 3 (above).

2. Licensee reserves the right to terminate the Licence in the event that payment is not received in full or if there has been a breach of this agreement by you.

Appendix 1 — Acknowledgements:

For Journal Content:
Reprinted by permission from [**the Licensor**]: [**Journal Publisher** (e.g. Nature/Springer/Palgrave)] [**JOURNAL NAME**] [**REFERENCE CITATION** (Article name, Author(s) Name), [**COPYRIGHT**] (year of publication)
For **Advance Online Publication papers:**
Reprinted by permission from [**the Licensor**]: [**Journal Publisher** (e.g. Nature/Springer/Palgrave)] [**JOURNAL NAME**] [**REFERENCE CITATION** (Article name, Author(s) Name), [**COPYRIGHT**] (year of publication), advance online publication, day month year (doi: 10.1038/sj.[JOURNAL ACRONYM].)
For Adaptations/Translations:
Adapted/Translated by permission from [**the Licensor**]: [**Journal Publisher** (e.g. Nature/Springer/Palgrave)] [**JOURNAL NAME**] [**REFERENCE CITATION** (Article name, Author(s) Name), [**COPYRIGHT**] (year of publication)
Note: For any republication from the British Journal of Cancer, the following credit line style applies:
Reprinted/adapted/translated by permission from [**the Licensor**]: on behalf of Cancer Research UK: : [**Journal Publisher** (e.g. Nature/Springer/Palgrave)] [**JOURNAL NAME**] [**REFERENCE CITATION** (Article name, Author(s) Name), [**COPYRIGHT]** (year of publication)
For **Advance Online Publication** papers:
Reprinted by permission from The [**the Licensor**]: on behalf of Cancer Research UK: [**Journal Publisher** (e.g. Nature/Springer/Palgrave)] [**JOURNAL NAME**] [**REFERENCE**

CITATION (Article name, Author(s) Name), [**COPYRIGHT**] (year of publication), advance online publication, day month year (doi: 10.1038/sj.[JOURNAL ACRONYM])

For Book content:

Reprinted/adapted by permission from [**the Licensor**]: [**Book Publisher** (e.g. Palgrave Macmillan, Springer etc) [**Book Title**] by [**Book author**(s)] [**COPYRIGHT**] (year of publication)

Other Conditions: Downloadable CAD and Code files included in the licence terms

Version 1.2

Questions? customercare@copyright.com or +1-855-239-3415 (toll free in the US) or +1-978-646-2777.

Supplemental Coding & CAD Files

Click here to access/download
Supplemental Coding Files
Codes and CADs.7z